

Durham Research Online

Deposited in DRO:

14 January 2020

Version of attached file:

Accepted Version

Peer-review status of attached file:

Peer-reviewed

Citation for published item:

Rotich, K.E. and Handler, M.R. and Naeher, S. and Selby, D. and Hollis, C.J. and Sykes, R. (2020) 'Re-Os geochronology and isotope systematics, and organic and sulfur geochemistry of the middle-late Paleocene Waipawa Formation, New Zealand : insights into early Paleogene seawater Os isotope composition.', *Chemical geology*, 536 . p. 119473.

Further information on publisher's website:

<https://doi.org/10.1016/j.chemgeo.2020.119473>

Publisher's copyright statement:

© 2020 This manuscript version is made available under the CC-BY-NC-ND 4.0 license
<http://creativecommons.org/licenses/by-nc-nd/4.0/>

Use policy

The full-text may be used and/or reproduced, and given to third parties in any format or medium, without prior permission or charge, for personal research or study, educational, or not-for-profit purposes provided that:

- a full bibliographic reference is made to the original source
- a [link](#) is made to the metadata record in DRO
- the full-text is not changed in any way

The full-text must not be sold in any format or medium without the formal permission of the copyright holders.

Please consult the [full DRO policy](#) for further details.

Re-Os geochronology and isotope systematics, and organic and sulfur
geochemistry of the middle–late Paleocene Waipawa Formation, New Zealand:
Insights into early Paleogene seawater Os isotope composition

Enock K. Rotich^{a*}, Monica R. Handler^a, Sebastian Naeher^b, David Selby^{c,d},
Christopher J. Hollis^b, Richard Sykes^b

^a *School of Geography, Environment and Earth Sciences, Victoria University of Wellington,
PO Box 600, Wellington, 6140, New Zealand*

^b *GNS Science, 1 Fairway Drive, PO Box 30368, Lower Hutt, 5040, New Zealand*

^c *Department of Earth Sciences, Durham University, Durham, DH1 3LE, UK*

^d *State Key Laboratory of Geological Processes and Mineral Resources, School of Earth
Resources, China University of Geosciences, Wuhan, 430074, Hubei, China*

* Corresponding author. Tel.: +64221308410; e-mail address: enock.rotich@vuw.ac.nz

Abstract

In the middle–late Paleocene, a marine, organic-rich sedimentary unit (Waipawa Formation [Fm]) in which the organic matter was derived mainly from terrestrial plants was deposited in many of New Zealand’s sedimentary basins. The unique organofacies of this formation has not been identified in any other time interval within the geological history of the Southwest Pacific, indicating that unusual climatic and oceanographic conditions likely prevailed during this time. It has, therefore, attracted wide scientific interest due to its significance for regional and global reconstruction of the early Paleogene transitional climate as well as potential for oil and gas production. Scarcity of age-diagnostic fossils, presence of unconformities and lack of volcanic interbeds have, however, hindered precise dating and correlations of all the known occurrences of the formation. Here, rhenium-osmium (Re-Os) geochronology has yielded the first radiometric age for the formation (57.5 ± 3.5 Ma), which is consistent with available biostratigraphic age determinations (59.4–58.7 Ma). Further, a comparison of Re-Os, bulk pyrolysis, sulfur and palynofacies data for the Waipawa Fm with those of more typical marine sediments such as the underlying Whangai Fm supports the interpretation that the chelating precursors or fundamental binding sites responsible for uptake of Re and Os are present in all types of organic matter, and that these elements have a greater affinity for organic chelating sites than for sulfides. The results also indicate that sedimentation rate may not play a dominant role in enhanced uptake of Re and Os by organic-rich sedimentary rocks.

The initial $^{187}\text{Os}/^{188}\text{Os}$ values for the Waipawa (~ 0.28) and Whangai (~ 0.36) formations are broadly similar to those reported for coeval pelagic sediments from the central Pacific Ocean, further constraining the low-resolution marine $^{187}\text{Os}/^{188}\text{Os}$ record of the Paleocene. We present a compilation of $^{187}\text{Os}/^{188}\text{Os}$ values from

organic-rich sedimentary rocks spanning the period between 70 and 50 Ma which shows that seawater Os gradually became less radiogenic from the latest Cretaceous, reaching a minimum value in the earliest late Paleocene (~59 Ma) during the deposition of Waipawa Fm, and then increased through the later Paleocene and into the early Eocene. The composite Os isotope record broadly correlates with global temperature ($\delta^{18}\text{O}$ and TEX_{86}) and carbon isotope ($\delta^{13}\text{C}$) records from the middle Paleocene to early Eocene, which is inferred to reflect climate-modulated changes in continental weathering patterns.

Keywords:

Re-Os geochronology; Waipawa Formation; New Zealand; Paleocene; seawater Os curve

1. Introduction

Marine organic-rich sediments are important archives of past climatic, oceanographic and geodynamic events. The Waipawa Fm is one such organic-rich sedimentary unit that has attracted considerable attention due to its significance for the early Paleogene climate reconstructions of the Southwest Pacific (e.g., Killops et al., 2000; Hollis et al., 2012; 2014; Hines et al., 2019), as well as its potential as a petroleum source rock (Moore, 1988; 1989; Killops et al., 1997; 2000; Schiøler et al., 2010; Field et al., 2018; Naeher et al., 2019). The formation contains a distinctive organofacies, termed the 'Waipawa organofacies', that is dominated by woody phytoclasts despite also showing a high abundance of marine C_{30} steranes and a heavy carbon isotope ($\delta^{13}\text{C}$) signature (values of -24 to -16‰) (Killops et al., 2000; Schiøler et al., 2010; Hollis et al., 2014; Field et al., 2018; Naeher et al., 2019). The

formation was deposited over a wide geographic extent covering multiple sedimentary basins around New Zealand and reaching as far west as the eastern margin of Tasmania (Fig. 1a; Schiøler et al., 2010; Hollis et al., 2014). The widespread deposition of such an unusual organic-rich sediment could only have resulted from a perturbation in Earth's oceanographic and climatic system (Killops et al., 2000; Schiøler et al., 2010; Hollis et al., 2014; Hines et al., 2019). However, it has not been established whether all known occurrences of Waipawa organofacies are coeval. This is because precise dating of the formation through biostratigraphy has so far been complicated by several factors, such as the presence of unconformities, scarcity of age-diagnostic fossils, poor age control for dinoflagellate datums, varying geochemical signatures between sections, and lack of reliable paleomagnetic data (Hollis et al., 2014). The Waipawa Fm and correlated units also lack interbedded volcanic beds that could potentially be used for radiometric dating. Available biostratigraphy and magnetostratigraphy from the East Coast Basin, New Zealand, place the timing of deposition of the formation in the late middle to early late Paleocene, spanning the Selandian–Thanetian boundary (Crouch et al., 2014; Hollis et al., 2014). Here, we investigate the potential of using the Re-Os isotope system to independently verify this age range and establish whether correlative units from other sedimentary basins are coeval.

Rhenium and Os are organophilic trace metals that become enriched in organic-rich sedimentary rocks (e.g., Ravizza and Turekian, 1989; Cohen et al., 1999; Selby and Creaser, 2003 and references therein). The resulting combination of high and variable Re and Os concentrations with variations in $^{187}\text{Re}/^{188}\text{Os}$ positively correlating with $^{187}\text{Os}/^{188}\text{Os}$ values means that the Re-Os isotope system can be used to directly obtain precise (in some cases, <1% uncertainty) and accurate ages of a wide variety

of organic-rich rocks including: marine shales (e.g., Ravizza and Turekian, 1989; Cohen et al., 1999; Selby and Creaser, 2005b; Kendall et al., 2006; Selby, 2007; Kendall et al., 2009b; Xu et al., 2009; Georgiev et al., 2011; Georgiev et al., 2017; Tripathy et al., 2018), lacustrine mudstones (Creaser et al., 2008; Poirier and Hillaire-Marcel, 2011; Cumming et al., 2012; Xu et al., 2017), and marine-influenced coals (Tripathy et al., 2015). Previous studies have also shown that post-depositional processes such as greenschist metamorphism and flash pyrolysis associated with igneous intrusions do not appreciably disturb the Re-Os isotope system (Creaser et al., 2002; Kendall et al., 2004; Yang et al., 2009; Rooney et al., 2011; Bertoni et al., 2014). In addition, the Re-Os isotope system remains closed during thermal maturation of organic matter and hydrocarbon generation (Creaser et al., 2002; Selby and Creaser, 2003). Based on these points, the Re-Os system represents an ideal geochronological tool to constrain the age of the Waipawa Fm. However, our current understanding of the exact mechanisms that control enrichment and fractionation of Re and Os in organic-rich sediments remains limited. For instance, despite the strong geochemical affinity that the elements have for organic matter, direct relationships between total organic carbon (TOC) content and Re and Os concentrations are not always evident; some sediments with high TOC may have low Re and Os concentrations and vice versa (Cohen et al., 1999; Kendall et al., 2004; Selby et al., 2009; Rooney et al., 2010). In addition, limited fractionation between Re and Os, and thus similar $^{187}\text{Re}/^{188}\text{Os}$ and $^{187}\text{Os}/^{188}\text{Os}$ compositions, has resulted in the production of imprecise ages (e.g., Turgeon et al., 2007; Selby et al., 2009; Rooney et al., 2011; Cumming et al., 2012; Bertoni et al., 2014). To further understand some of the factors controlling uptake and fractionation of Re and Os in sedimentary rocks, we have included the underlying Whangai Fm in our analyses because its organic matter

composition and depositional conditions appreciably differ from those of the Waipawa Fm.

In addition to geochronology, the Os isotope composition ($^{187}\text{Os}/^{188}\text{Os}$) of organic-rich sediments provide useful information about past climatic and oceanographic conditions (Ravizza et al., 2001; Schmitz et al., 2004; Peucker-Ehrenbrink and Ravizza, 2012; Du Vivier et al., 2014; Dickson et al., 2015). The Waipawa Fm was deposited during a prolonged temperature minimum in the mid-Paleocene (~60–58 Ma) prior to the start of progressive warming into the early Eocene. This trend is evident in both high-resolution deep-sea oxygen and carbon isotope records (Westerhold et al., 2011; Littler et al., 2014; Barnet et al., 2019) as well as regional sea surface temperatures (58–53 Ma; Bijl et al., 2009; Hollis et al., 2012, 2014). The deposition of the formation also corresponds with the first phase of a positive $\delta^{13}\text{C}$ excursion (~59–57 Ma; Westerhold et al., 2011; Littler et al., 2014; Barnet et al., 2019), which is interpreted to reflect a time of enhanced carbon burial, either as marine (Corfield and Cartlidge, 1992) or terrestrial organic matter (Kurtz et al., 2003). Shifts in $\delta^{13}\text{C}$ of marine organic-rich rocks have also been linked to changes in the rate of oxidative weathering of organic matter buried in continents (Ravizza, 1993; Ravizza and Esser, 1993; Ravizza et al., 2001; Percival et al., 2016; Them et al., 2017; De Lena et al., 2019). The marine Os isotope record can track globally-averaged variations in continental weathering fluxes because at any point in time, the record reflects the balance between radiogenic Os weathered from the continent ($^{187}\text{Os}/^{188}\text{Os} = \sim 1.4$) and non-radiogenic Os from hydrothermal activities and extra-terrestrial materials ($^{187}\text{Os}/^{188}\text{Os} = 0.12$) (Peucker-Ehrenbrink and Ravizza, 2000; Cohen, 2004). The residence time of Os in the water column (10–50 ka range, sometimes <10 ka) is also short enough to respond to short-term variations in input

but sufficiently long to allow homogenization of the Os signature in the global ocean
 (Burton et al., 1999; Cohen, 2004; Du Vivier et al., 2014; 2015; Rooney et al., 2016).
 The seawater Os record for much of the Paleocene, however, remains poorly
 resolved (Peucker-Ehrenbrink and Ravizza, 2012). The few available $^{187}\text{Os}/^{188}\text{Os}$
 data for this period are also based on analyses of pelagic clay sequences (Pegram
 and Turekian, 1999) and Fe-Mn crusts (Klemm et al., 2005) which have numerical
 age models that are not easily correlated with those of marine organic-rich
 sedimentary rocks because they are based on coarse resolution ichthyolith
 biostratigraphy and empirical growth rates of hydrogenous cobalt (Peucker-
 Ehrenbrink and Ravizza, 2012). These analyses are also based on a leaching
 method that may not have preferentially isolated the hydrogenous component of Os,
 possibly recording inaccurate seawater Os composition due to the potential presence
 of detrital Os (Pegram and Turekian, 1999; Peucker-Ehrenbrink and Ravizza, 2012).
 Nonetheless, the pelagic clay record hints at seawater Os with low $^{187}\text{Os}/^{188}\text{Os}$
 values of around 0.26–0.32 from around 57–61 Ma, but the extent and cause of
 these non-radiogenic $^{187}\text{Os}/^{188}\text{Os}$ values remain unclear due to the low resolution of
 the record (Pegram and Turekian, 1999; Peucker-Ehrenbrink and Ravizza, 2012).
 Here, we present Re-Os elemental and isotope compositions and bulk pyrolysis and
 sulfur data for the Waipawa and Whangai formations from the Wairarapa and
 Hawke's Bay region of the East Coast Basin, New Zealand (Fig. 1a). One additional
 Waipawa Fm sample from the North Slope Basin was included to assess Re-Os
 abundance and isotopic composition of Waipawa organofacies beyond the East
 Coast Basin (Fig. 1a). These data allow us to constrain the depositional age of the
 Waipawa Fm and contribute to further understanding of mechanistic controls of Re-
 Os systematics in organic-rich sedimentary rocks. In addition, the Os isotope data of

the Waipawa and Whangai formations are included in a compilation of initial $^{187}\text{Os}/^{188}\text{Os}$ (Os_i) ratios for sedimentary rocks that span the latest Cretaceous to early Eocene (70–50 Ma), enabling us to evaluate temporal trends in Os geochemical cycle during this period.

2. Geological setting

The focus of this study is on the Waipawa and Whangai formations from the East Coast Basin, New Zealand, which extends from East Cape in North Island to the Kaikoura Peninsula in South Island, and about half of which is offshore (Fig. 1a). The basin occupied a site on the Pacific subduction margin of Gondwana during the Triassic to early Cretaceous time when rocks of Torlesse Terrane (greywacke) were accreted to form the now weakly metamorphosed and deformed mudstone and sandstone basement (Field et al., 1997; King, 2000). From the mid-Cretaceous, the basin transitioned into a northward-prograding, passive continental margin (Fig. 1b) that allowed thick units of Late Cretaceous to Paleogene sediments, eroded from axial ranges, to be deposited onto the continental shelf and slope (King, 2000). The propagation of the modern plate boundary in the early Miocene transformed the setting of the basin from a passive margin to a convergent forearc basin (King, 2000). The additional one sample (Blacks Quarry) from Northland is from an allochthonous sequence, which is inferred to have originated in the North Slope Basin (Fig. 1a, b; Hollis et al., 2006).

The Waipawa Fm is a poorly bedded, brownish black, organic-rich marine sedimentary unit that ranges in thickness from ~2 to 80 m (Moore, 1988; Hollis et al., 2014; Field et al., 2018; Naeher et al., 2019). Foraminiferal paleobathymetry indicates that the formation was deposited in an upper- to mid-slope setting (Field et

al., 2018; Naeher et al., 2019). Palynological and palynofacies data suggest that the Waipawa Fm and correlated units were deposited during a sea-level fall (Schiøler et al., 2010; Hollis et al., 2014 and references therein) within a relatively short period of time in the late Paleocene (ca. 0.7 My; Fig. 2; Hollis et al., 2014). The fall in sea-level is thought to have resulted in increased delivery of terrestrial organic matter to continental slope settings as the exposed nearshore and shelfal areas were largely bypassed (Hines et al., 2019; Naeher et al., 2019). Oscillations in key geochemical parameters (e.g., TOC, hydrogen index [HI], oxygen index [OI], $\delta^{13}\text{C}$ and palynofacies) through the formation indicate that influxes of terrestrial organic matter occurred episodically (Naeher et al., 2019). For the most part, the Waipawa Fm conformably overlies the Whangai Fm and the transition into Waipawa organofacies is gradational (Moore, 1989; Naeher et al., 2019). There is, however, an unconformity in some sections where the Waipawa Fm is condensed (Wilson and Moore, 1988; Hollis et al., 2014). The top of the formation is commonly marked by an unconformity (Schiøler et al., 2010; Hollis et al., 2014).

The Whangai Fm is a thick (typically 300–500 m), poorly bedded, variably calcareous and regionally extensive mudstone that consists of the Upper Calcareous, Rakauroa, Te Uri, Porangahau and Kirks Breccia members (Moore, 1988; Field et al., 1997). The Whangai Fm samples analysed in this study are all from the Upper Calcareous Member, which commonly underlies the Waipawa Fm in the East Coast Basin.

3. Samples and analytical methodology

3.1 Samples and sample preparation

Waipawa Fm samples were collected from the Orui-1A drill core, housed at the New Zealand National Core Store in Featherston, and archived outcrop samples from

Taylor White section and Blacks Quarry held at GNS Science. The Orui-1A stratigraphic drill hole was drilled in 2011 to a total depth of 117.3 m near Riversdale, coastal Wairarapa (41° 3' 54.36" S, 176° 5' 16.44" E; Fig. 1a; Field et al., 2018). Taylor White section is a road-side section exposed on Angora Road (40°27'46.9" S, 176°28'24.9" E), near the small settlement of Wimbledon, southern Hawke's Bay (Fig. 1a; Bland et al., 2014). This section was freshly exposed when road construction was undertaken to widen the Angora Road, allowing for fresh samples to be collected after several meters of rock had been removed (Bland et al., 2014; Naeher et al., 2019). Blacks Quarry is located in the Doubtless Bay, in the Northland region of North Island (34° 58' 40.62" S, 173° 23' 54.24" E, Fig. 1a). Whangai Fm samples were obtained from a collection of archived outcrop samples held at GNS Science, previously collected from the lower part of Angora Road (40°27'43.2" S, 176°28'42.2" E; Tayler, 2011; Hollis et al., 2014), termed the 'Angora Road section' in the present study. Stratigraphically, the Whangai Fm samples are located ca. 17–35 m below the base of Waipawa Fm (Tayler, 2011; Hollis et al., 2014). The Orui-1A samples were obtained from a 3.2 m stratigraphic interval between the depths of 48.4 and 51.6 m, with sample spacing ranging from 13 to 72 cm and each sample representing a stratigraphic interval of approximately 3 to 5 cm. Care was taken to avoid zones of faulting, brecciation and calcite veining that were present in the core. By contrast, the Taylor White samples are from a much thicker stratigraphic interval of approximately 50 m and were not collected specifically for Re-Os geochronology which requires that sampling to be done over a small stratigraphic interval to minimize possible variation in initial $^{187}\text{Os}/^{188}\text{Os}$ ratios (Cohen et al., 1999; Selby and Creaser, 2003; Kendall et al., 2009b). The Taylor White samples were included to examine how varying depositional conditions within the Waipawa Fm, as shown by

stratigraphic oscillations in key geochemical parameters (Naeher et al., 2019), may have affected the Re-Os systematics. A total of 23 samples are examined in this study; 18 from the Waipawa Fm and 5 from Whangai Fm.

Sample processing was undertaken in the rock crushing facility at Victoria University of Wellington (VUW). Rock samples (80–100 g) were polished to remove any surface contamination and drilling marks from the core material following the protocols of Kendall et al. (2009a). The samples were then dried in an oven overnight at 40 °C, broken into small pieces without direct metal contact, and powdered using an agate mill.

3.2 Bulk pyrolysis and sulfur analyses

Bulk pyrolysis and sulfur data obtained by this study were used in conjunction with published geochemical and palynofacies datasets (Naeher et al., 2019) to assess the variation in organic matter type and depositional conditions within the Waipawa and Whangai formations. Bulk pyrolysis analyses for the Orui-1A and Angora Road samples were undertaken at GNS Science following published methods (Naeher et al., 2019). In brief, powdered samples were analysed using a Weatherford Laboratories TOC/TPH Source Rock Analyser (SRA) to obtain key geochemical parameters that include TOC, total volatile (S1) and pyrolysable (S2) hydrocarbons, temperature of maximum pyrolysis yield (T_{max}), HI and OI. The temperature programme used was 300 °C isothermal for 3 min, then increased at a rate of 25 °C min⁻¹ to 650 °C (isothermal at 650 °C for 1 min) to pyrolyse the kerogen, followed by oxidation at 630 °C for 20 min. A standard (Institut Français du Pétrole [IFP] standard 160000) was run at the start and finish of each sample sequence, and after every 8 samples to check for data quality. Bulk pyrolysis data for the Taylor White samples

1
2
3
4
5
6
7
8
9
10
11
12
13
14
15
16
17
18
19
20
21
22
23
24
25
26
27
28
29
30
31
32
33
34
35
36
37
38
39
40
41
42
43
44
45
46
47
48
49
50
51
52
53
54
55
56
57
58
59
60
61
62
63
64
65

were obtained from Naeher et al. (2019). Bulk pyrolysis data for the Blacks Quarry sample were obtained previously from the Geological Survey of Canada, Calgary, using a Rock-Eval 6 instrument.

Analyses of total sulfur content (S_{tot}) and forms of sulfur for the Orui-1A, Angora Road and Blacks Quarry samples were undertaken by CRL Energy Ltd in Lower Hutt, New Zealand, using standard procedures (Naeher et al., 2019). In brief, S_{tot} was determined by high-temperature (1350 °C) tube furnace combustion, based on the ASTM Standard D4239 technique, using a Leco Truspec Sulfur Analyser model 630-100-700 (Naeher et al., 2019). The different forms of sulfur were determined according to Australian Standard AS1038.11-2002 where sulfate sulfur (S_{sul}) is extracted by 10% HCl and determined gravimetrically after purification and precipitation. The HCl extracted residue is then decomposed with nitric acid and oxidised using H_2O_2 to obtain pyritic iron. The pyritic iron is measured by atomic absorption spectroscopy and used to calculate pyritic sulfur (S_{pyr}). Organic sulfur (S_{org}) is obtained by subtracting the sum of S_{sul} and S_{pyr} from S_{tot} . Sulfur data for the Taylor White samples were available from Naeher et al. (2019) and were also analysed by CRL Energy Ltd using the same procedures and instrumentation.

3.3 Re-Os analyses

To enable optimisation for isotope dilution analyses, Re concentrations were first determined at the VUW geochemistry laboratory following protocols from Durham University as described in the supplementary online material (e.g., Jones et al., 2018). Full Re-Os isotope analyses of the samples were carried out at Durham University's laboratory for source rock and sulfide geochronology and geochemistry following previously published protocols for isolation, purification and measurement

by isotope dilution - negative thermal ionization mass spectrometry (e.g., Cumming et al., 2012; Jones et al., 2018). In brief, a known amount of rock powder (300–500 mg) was spiked with a known amount of $^{190}\text{Os} + ^{185}\text{Re}$ mixed tracer solution and digested using $\text{Cr}^{\text{VI}}\text{--H}_2\text{SO}_4$ solution in a sealed carius tube at 220 °C for 48 h. Osmium was separated and purified from the solution using solvent extraction and micro-distillation methods. The residual Re bearing solution was evaporated to dryness at 80 °C and purified by NaOH-acetone solvent extraction and further purified using HCl-HNO₃ anion exchange chromatography.

The resulting Re and Os fractions were loaded onto Nickel and Platinum wire filaments, respectively, and their isotopic compositions measured on a Thermo Scientific TRITON Negative Thermal Ionisation Mass Spectrometer housed at the Arthur Holmes Laboratory, Durham University. Rhenium isotopic composition was measured via static collection mode in Faraday cups, with Os measured via ion-counting through a secondary electron multiplier (SEM) in a peak-hopping mode. Total procedural blanks during this study were 14.6 ± 0.16 pg Re and 50 ± 0.01 fg Os, with an $^{187}\text{Os}/^{188}\text{Os}$ value of 0.22 ± 0.08 ($n = 4$). In-house standards for both Re (Restd; Selby, 2007) and Os (DROsS; Nowell et al., 2008) were run with every batch of samples to monitor instrument reproducibility and ensure data quality. The Re standard solution yields an average $^{185}\text{Re}/^{187}\text{Re}$ ratio of 0.59843 ± 0.00193 ($n = 7$) that is similar to the established natural $^{185}\text{Re}/^{187}\text{Re}$ ratio of 0.59739 ± 0.00039 (Gramlich et al., 1973), and was used to correct for mass fractionation in the measured Re data. The average $^{187}\text{Os}/^{188}\text{Os}$ ratio of the in-house Durham Romil Osmium Standard (DROsS) was 0.16089 ± 0.00056 ($n = 7$), consistent with values reported in previous studies from the same lab (e.g., Cumming et al., 2012; Liu and Selby, 2018, and references therein), and also in excellent agreement with values

reported by other laboratories (0.16078 ± 0.00024 , Liu and Pearson, 2014; 0.16091 ± 0.00015 , van Acken et al., 2019). The Re-Os isotopic data, calculated 2σ uncertainties for $^{187}\text{Re}/^{188}\text{Os}$ and $^{187}\text{Os}/^{188}\text{Os}$ and the associated error correlation function (rho; Ludwig, 1980), were regressed using the beta version of the Isochron program (Li et al., 2019) which incorporates the benchmark Isoplot algorithm (Ludwig, 2012) and a new approach that employs the Monte Carlo sampling method for error propagation. In the Isoplot program, a Model 1 age assumes that the assigned 2σ uncertainties and calculated error correlations are the only reason the data-points scatter from the regression line whereas a Model 3 age assumes that the scatter about the isochron line may be linked to both the assigned analytical errors and other geological factors that produce variation in the initial $^{187}\text{Os}/^{188}\text{Os}$ values (Ludwig, 2012). The Isoplot program separates the two scenarios based on the probability of how well the data fit the regression line. By contrast, the Monte Carlo method makes no prior assumption about the possible causes of scatter in the geochronological results and propagates uncertainties (2σ) from both analytical measurements and model assumptions in a consistent manner irrespective of the probability of fit (Li et al., 2019).

4. Results and discussion

4.1 Kerogen type and maturity

The bulk pyrolysis data for the Orui-1A, Taylor White and Angora Road samples (Table 1; Fig. 3) are consistent with published results for the Waipawa and Whangai formations in the East Coast Basin (Tayler, 2011; Field et al., 2018; Naeher et al., 2019). The TOC within the Waipawa Fm in the Orui-1A core and Taylor White section is highly variable, generally ranging from 0.4–5 wt.% with a mean of 2.2 wt.%

(Fig. 3a; Naeher et al., 2019). TOC is very high (~10 wt.%) in the Blacks Quarry sample from the North Slope Basin (Fig. 3a). By contrast, the Whangai Fm at Angora Road exhibits low TOC content (mostly <1 wt.%, Fig. 3a). All samples presented here are thermally immature as indicated by T_{\max} values ranging from 396–428 °C (Fig. 3b; Tissot and Welte, 1984), and thus, the observed kerogen types within the two formations are representative of the initial kerogen types which, based on the modified van Krevelen diagram (Fig. 3c), varies from Type II to Type III. The wide variations in T_{\max} , HI and OI values displayed by the Waipawa Fm samples in the complete Taylor White sample set in Fig. 3b and c are a result of stratigraphic variations in kerogen type, in part resulting from changing redox conditions within the depositional environment, rather than to variations in maturity or sample weathering (Field et al., 2018; Naeher et al., 2019). Similar stratigraphic variations in kerogen type also occur within the Waipawa Fm in the Orui-1A core (Field et al., 2018), but are not reflected amongst the Orui-1A samples because these were selected from a thin (3.2 m) stratigraphic interval with relatively uniform T_{\max} , HI and OI values. In both the Taylor White Section and Orui-1A core, OI is consistently low (≤ 50 mg CO₂/g TOC) in the upper part of the Waipawa Fm despite high variability in TOC, S₂, and HI (Field et al., 2018; Naeher et al., 2019). Palynofacies analyses indicate that the organic matter in the Waipawa Fm is mainly terrestrial woody plant matter whereas marine-sourced amorphous organic matter dominates in the Whangai Fm (Field et al., 2018; Naeher et al., 2019).

4.2 Re and Os concentrations

The Waipawa Fm samples from Orui-1A core, Taylor White section and Blacks Quarry are all enriched in both Re (22.5–85.9 ppb) and Os (397.9–598.6 ppt [¹⁹²Os 153.8–254.9]; Table 2) relative to the average concentrations of these elements in

the upper continental crust (0.2–2 ppb Re and 30–50 ppt Os; Esser and Turekian, 1993; Sun et al., 2003). The Whangai Fm samples from the Angora Road section are only slightly enriched in Re (3.6–11.8 ppb) and Os (141.8–228.1 ppt [^{192}Os 55.4–89.0]) compared to the upper continental crust. Three Waipawa Fm samples from the Taylor White section are particularly enriched in Re (TW-17 = 85.9 ppb, TW-29 = 72.9 ppb and TW-51 = 56.3 ppb). The high and variable Re concentrations in the Waipawa Fm, especially in the Taylor White samples (Table 2), may indicate some form of water mass restriction with varying degrees of replenishment of the water column by Re-rich water from the open ocean (McArthur et al., 2008; van Acken et al., 2019). This is supported by biomarker evidence which suggests that there was persistent water column stratification during the deposition of the formation in the East Coast Basin (Naeher et al., 2019), as well as suggestions of restricted shallow marine depositional setting for Waipawa organofacies in other sedimentary basins such as the Great South and Canterbury basins (Schjølter et al., 2010). Sample TW-17 and TW-29 show elevated OI values of 131 mg CO₂/g TOC and 68 mg CO₂/g TOC, respectively, compared to the other Taylor White samples studied here, which are very consistent between 25 and 29 mg CO₂/g TOC (Table 1, Fig. 3c). This suggests that these two samples either contain different types of organic matter or they have been affected by oxidative weathering. The latter appears more likely since Re-Os isotope data for the two samples also yield negative initial $^{187}\text{Os}/^{188}\text{Os}$ (Os_i) values (Table 2), which has been suggested to indicate disturbance to the Re-Os system through oxidative weathering (Jaffe et al., 2002; Georgiev et al., 2012). We therefore treat these two samples as outliers and exclude them from further discussion.

4.3 Re and Os uptake and fractionation in the Waipawa and Whangai formations

The association of Re and Os with TOC and sulfur may provide useful information on the depositional conditions that enhance the uptake of these elements into organic-rich sediments (Cohen et al., 1999; Cumming et al., 2012; Georgiev et al., 2012; Rooney et al., 2012). Strong positive correlations exist between TOC and Re ($R^2 = 0.91$) and ^{192}Os ($R^2 = 0.73$) in the Orui-1A samples (Fig. 4a, b), suggesting an uptake mechanism that is linked to the abundance of organic matter (e.g., Georgiev et al., 2012; Rooney et al., 2012 and references therein). The ^{192}Os isotope is plotted to avoid the effects of radiogenic in-growth of ^{187}Os , allowing for direct comparison of hydrogenous Os concentrations in the different samples. Samples from the Taylor White section show no significant correlation between TOC and Re ($R^2 = -0.04$) and ^{192}Os ($R^2 = 0.08$) (Fig. 4a, b), which may indicate possible effects of surficial weathering in these outcrop samples. The apparent correlations between TOC and Re and Os concentrations in the Angora Road samples may be spurious because they rely on one sample that plots away from the other clustered samples (Fig. 4a, b). In general, the Waipawa Fm, with higher TOC content, exhibits higher concentrations of Re and Os than the Whangai Fm (Fig. 4a, b). The large proportion of terrestrial organic matter (66 to 98% degraded phytoclasts) in the Waipawa Fm (Schjøler et al., 2010; Hollis et al., 2014; Field et al., 2018; Naeher et al., 2019) does not appear to have impacted the uptake of Re and Os, supporting previous interpretations that chelating precursors or fundamental binding sites responsible for the uptake of Re and Os are present in all types of organic matter (Cumming et al., 2012; Harris et al., 2013; Du Vivier et al., 2015). The difference in concentrations of Re and Os in the two formations might also be a factor of the abundance, variability and preservation of organisms such as macroalgae that are components of

sedimentary organic matter and which have recently been shown to accumulate Re (up to several hundreds of ppb) and Os (Racionero-Gómez et al., 2016; Rooney et al., 2016; Racionero-Gómez et al., 2017; Ownsworth et al., 2019). The accumulation of Re by macroalgae has been shown to be syn-life and unidirectional i.e. once the living macroalgae absorb Re, it does not release it back to the water (Racionero-Gómez et al., 2016). However, the study also suggests that Re may be released back to the water column once the macroalgae die and break down, and that depositional conditions which prevent or lower the rate of macroalgal degradation (such as anoxia and low temperature) may be required for much of the accumulated Re to be incorporated into sediments (Racionero-Gómez et al., 2016). The hypoxic conditions during the deposition of the Waipawa Fm, compared to the oxic conditions in the Whangai Fm (Naeher et al., 2019), might therefore be the reason for its higher Re and Os concentrations.

The Waipawa Fm is enriched in S_{tot} (1.25–2.31 wt.%) compared to the Whangai Fm (0.72–0.85 wt.%) (Fig. 5a, b), suggesting deposition under less oxic conditions (Didyk et al., 1978; Georgiev et al., 2012; Naeher et al., 2019). S_{tot} is also positively correlated with the abundance of Re ($R^2 = 0.84$) and ^{192}Os ($R^2 = 0.72$), as well as the $^{187}\text{Re}/^{188}\text{Os}$ ratio ($R^2 = 0.66$) in samples from this study (Fig. 5a, b, c). This may suggest that the uptake and fractionation of Re and Os are linked to the redox conditions of the depositional environment (Colodner et al., 1993; Crusius et al., 1996; Cohen et al., 1999; Morford and Emerson, 1999; Crusius and Thomson, 2000; Yamashita et al., 2007; Georgiev et al., 2011). However, no simple correlation can be established between Re and Os concentrations and other indicators of redox conditions such as HI and OI (Table 1). The sulfur speciation data [normalised to S_{tot} as there is a high variation in S_{tot} within the Waipawa Fm (Naeher et al., 2019)] also

show that only organic sulfur ($S_{\text{org}}/S_{\text{tot}}$) exhibits strong positive correlations with Re ($R^2 = 0.75$; Fig. 6a) and ^{192}Os ($R^2 = 0.77$; Fig. 6b) concentrations compared to pyritic sulfur ($S_{\text{pyr}}/S_{\text{tot}}$) and sulfate sulfur ($S_{\text{sul}}/S_{\text{tot}}$), which exhibit negative (Re $R^2 = -0.68$; ^{192}Os $R^2 = -0.80$; Fig. 6c, d) and weak-positive (Re $R^2 = 0.25$; ^{192}Os $R^2 = 0.39$; Fig. 6e, f) correlations, respectively. This supports previous findings that suggested that Re and Os have a greater affinity for organic chelating sites than sulfides (Cohen et al., 1999; Rooney et al., 2012).

Slow sedimentation, which increases the time of exposure of organic matter to the sediment-water interface, is another factor that has been considered to play an important role in enhanced uptake of Re and Os in organic-rich sedimentary rocks (Lewan and Maynard, 1982; Selby et al., 2009; Cumming et al., 2012; Rooney et al., 2012). The average sedimentation rate for the Waipawa Fm (~10.6 cm/ky) is almost an order of magnitude higher than that of the Whangai Fm (~1.1 cm/ky) (Naeher et al., 2019), and also significantly higher than those of several other marine organic-rich rocks previously dated with the Re-Os isotope system (<2 cm/ky) (e.g., Kendall et al., 2009b; Georgiev et al., 2017; Tripathy et al., 2018). Therefore, if slow sedimentation rate plays a primary control in Re and Os uptake in organic-rich sediments, then the Waipawa Fm would be expected to record low levels of Re and Os. Instead, the average concentrations of Re (38.9 ppb) and ^{192}Os (192.6 ppt) in the Waipawa Fm are approximately 6 and 3 times higher, respectively, than those of Whangai Fm (Re = 6.6 ppb; ^{192}Os = 65.6 ppt), indicating that, in this instance, slower sedimentation rates have not had a significant impact on sequestration of Re and Os. The relatively low levels of Re and Os in the Whangai Fm, compared to the Waipawa Fm, may simply be a factor of its low TOC content and different depositional conditions. However, the Re and Os concentrations in the Waipawa Fm are

comparable to those reported for other marine shales with similar geochemical characteristics, albeit with much lower sedimentation rates. For example, the Upper Jurassic Hekkingen Fm with TOC of 3.08–10.9 wt.%, Type II/III kerogen, anoxic depositional conditions and a sedimentation rate of 1.83 cm/ky has average Re and ^{192}Os abundances of 46 ppb and 158.4 ppt, respectively, similar to those of the Waipawa Fm (Langrock and Stein, 2004; Georgiev et al., 2017; Tripathy et al., 2018). Therefore, based on these results, it appears that a slow sedimentation rate does not play a significant role in Re and Os enrichment in organic-rich sediments, at least in the range from 1.1 cm/ky to 10.6 cm/ky. This argument is supported by previous studies which suggested that the oxidation effects brought about by a slow sedimentation rate lead to poor preservation of organic matter (Ingall and Cappellen, 1990) and subsequent re-immobilization (precipitation) of Re (Crusius and Thomson, 2000).

4.4 Re-Os geochronology of the Waipawa Formation

The $^{187}\text{Re}/^{188}\text{Os}$ values of samples from the Orui-1A core range from 256.4 to 345.1 and are positively correlated to the $^{187}\text{Os}/^{188}\text{Os}$ values, which range from 0.527 to 0.612 (Fig. 7a). Regression of the isotope data using the Isoplot algorithm yields a Model 3 isochron age of 58.1 ± 3.9 Ma ($n = 9$; Mean Square of Weighted Deviates [MSWD] = 4.1), with an Os_i of 0.28 ± 0.02 (Fig. 7a). When the Monte Carlo method is used, the age (58.1 ± 4.4 Ma) and Os_i (0.28 ± 0.02) are the same as those of the Isoplot method, except that the age uncertainty is slightly greater in the Monte Carlo method due to a higher percentage of the uncertainties (61%) being related to the model age calculation (Li et al., 2019; Fig. 7b). Precise Re-Os dating of sedimentary rocks requires that: 1) the initial $^{187}\text{Os}/^{188}\text{Os}$ ratios (Os_i) are identical, 2) there is a sufficient spread in $^{187}\text{Re}/^{188}\text{Os}$ ratios of at least a few hundred units, and 3) the Re-

Os system remains undisturbed (Cohen et al., 1999; Selby and Creaser, 2005a). The obtained Os_i values for Orui-1A samples are all nearly identical, ranging from 0.277–0.286, with a mean of 0.280 ± 0.002 (1SD; Table 2). Only sample Orui-11e shows a slightly larger deviation from the mean Os_i (0.006) and as a result, exhibits the largest standard error of prediction (0.92%) from the line of best-fit through the data (Fig. 7a). Analytical uncertainties, variation in the composition of Os during deposition and post-depositional processes such as brecciation and calcite veining that were present in the core are some of the possible reasons for the variance in the Os_i of sample Orui-11e. Regression of the Re-Os data without this sample (Orui-11e) using the Isoplot program yields a more precise Model 1 age of 57.4 ± 1.7 Ma ($Os_i = 0.28 \pm 0.01$, $n = 8$, MSWD = 1.5; Fig. 7c). In comparison, the Monte Carlo method yields an age of 57.5 ± 3.5 Ma ($Os_i = 0.28 \pm 0.02$; Fig. 7d), which indicates that the Model 1 scenario of the Isoplot program underestimated the age uncertainties by ~50%. We suggest that the larger uncertainties in the obtained Re-Os age may be a result of the limited spread in both $^{187}Re/^{188}Os$ (80 units) and $^{187}Os/^{188}Os$ (0.085 units) displayed by the Orui-1A samples, in addition to uncertainties from analytical measurements (Selby et al., 2009; Rooney et al., 2017; Li et al., 2019). Small ranges in Re-Os ratios have also been reported for other marine and lacustrine organic-rich rocks (Turgeon et al., 2007; Selby et al., 2009; Finlay et al., 2010; Cumming et al., 2012; Zhu et al., 2013; Tripathy et al., 2018) where a lack of variability in organic matter type coupled with a relatively homogenous depositional environment (Cumming et al., 2012) and redox conditions that drawdown Re relative to Os (Turgeon et al., 2007) were suggested as the main reasons for the low spread in Re-Os ratios. A lack of variability in organic matter type is a feature of the Waipawa Fm, especially in the

Orui-1A samples, possibly explaining the observed similarity in the Re-Os ratios of these samples.

The $^{187}\text{Re}/^{188}\text{Os}$ ratios of samples from the Taylor White section range from 283.7 to 498.9 (excluding the two outliers discussed in Section 4.2) and are positively correlated with their corresponding $^{187}\text{Os}/^{188}\text{Os}$ values, which range from 0.551 to 0.767 (Fig. 8a). Regression of the isotope data yields a Re-Os date of 58.3 ± 7.7 Ma ($\text{Os}_i = 0.29 \pm 0.05$; MSWD = 28.8) using the Isoplot algorithm and 58.3 ± 6.5 Ma ($\text{Os}_i = 0.29 \pm 0.04$; $n = 6$) using the Monte Carlo method (Fig. 8a, b). These Re-Os dates agree well with those derived from the Orui-1A samples, but with larger uncertainties. The high MSWD value associated with the Re-Os date from the Isoplot program, relative to the ideal value of ~ 1 , indicates that the final age uncertainty is controlled by both analytical and geological uncertainties (Ludwig, 2012). This might be expected given the large stratigraphic interval that the samples represent. However, the whole ~ 80 m of Waipawa Fm in the Taylor White section is estimated to have been deposited within a relatively short period of time (~ 700 ky; Hollis et al., 2014; Naeher et al., 2019) and thus, temporal variation in Os_i is deemed unlikely to fully explain the uncertainty in the obtained Re-Os date. An alternative explanation is that the episodic influxes of large amounts of terrestrial material during deposition of the formation in the Taylor White section (Naeher et al., 2019) may have supplied high loads of continental-derived Os that introduced localised variation in seawater Os_i . Further, the oxidative weathering that affected the Re-Os systematics of the two outlier samples discussed above (Section 4.2) may have also caused subtle effects in the other Taylor White samples.

4.5 Comparison of the Waipawa Formation Re-Os and biostratigraphic ages

Dating the Waipawa Fm through biostratigraphy has been challenging mainly due to poor preservation and scarcity of age-diagnostic fossils. For example, the boundaries of dinoflagellate (NZDP) or calcareous nannofossil (NP) zones were not precisely located in the Orui-1A core due to the scarcity of fossils (Field et al., 2018). The interval of the Orui-1A core sampled in the present study (48.4 to 51.6 m) is also barren of nannofossils and thus, lacks precise age constraints. However, the base of the overlying Wanstead Fm, at 36.84 m, is assigned to Zones NZDP8 and NP8 while the top of Zone NZDP7 is placed at 75.88 m (Fig. 2), which indicates that the Orui-1A samples studied here are of earliest late Paleocene age (~59 Ma). Dinocyst assemblages from several sections in eastern New Zealand indicate that the Waipawa Fm can be correlated with an interval that extends from upper Zone NZDP7 to lower NZDP8 (Crouch et al., 2014; Hollis et al., 2014). Nannofossil biostratigraphy for the Angora Road section also indicates that the Waipawa Fm is correlated with an interval that spans lowermost Zone NP6 to upper Zone NP7 (Fig. 2; Hollis et al., 2014). This biostratigraphy was combined with age control from other sections to infer that the Waipawa Fm was deposited over a short period of time (~700 ky) during the late middle to early late Paleocene (59.4 to 58.7 Ma; Hollis et al., 2014). The Re-Os depositional age for the Waipawa Fm obtained from the Orui-1A samples (57.5 ± 3.5 Ma) overlaps with this biostratigraphic age, effectively providing the first direct radiometric age constraint for this formation.

4.6 Re-Os depositional age of the Whangai Formation

The $^{187}\text{Re}/^{188}\text{Os}$ ratios in the Whangai Fm samples from the Angora Road section range from 121.1 to 264.7 and correlate positively with the $^{187}\text{Os}/^{188}\text{Os}$ ratios, which

range from 0.484 to 0.633 (Fig. 8c). Regression of the isotope data yields imprecise Re-Os date of 61.9 ± 17.8 Ma ($Os_i = 0.36 \pm 0.06$; $n = 5$; MSWD = 79.7) using the Isoplot algorithm (Fig. 8c) and 61.9 ± 13.5 Ma ($Os_i = 0.36 \pm 0.05$) using the Monte Carlo method (Fig. 8d). The large uncertainties in the Re-Os date for these samples reflect the likely variations in Os_i over the relatively large time period (~ 2 Ma) represented by the ~ 17 m stratigraphic thickness covered by the Angora Road samples (Kendall et al., 2009b). Over this interval, Os_i varies from 0.343–0.369 and tends to become lower up-section, consistent with an overall decreasing trend in Os_i from the lowest Whangai Fm sample (0.369) to the highest Waipawa Fm sample in the Taylor White section (0.285). Despite the Re-Os date for the Angora Road samples being imprecise, the mean value of 61.9 Ma is in good agreement with the published age model for the section (Hollis et al., 2014), which combines both calcareous nannofossil and dinoflagellate biostratigraphy (Crouch et al., 2014; Kulhanek et al., 2015), to infer an age range of ~ 62 to 61 Ma for the sampled interval.

4.7 Middle–late Paleocene seawater Os isotope composition

The Os_i ratio derived from regression of Re-Os data is interpreted to record the Os isotope composition of the seawater at the time of deposition (Ravizza and Turekian, 1989; Cohen et al., 1999; Selby and Creaser, 2003; Selby et al., 2009). The isochron-derived Os_i values for the Waipawa Fm in Orui-1A (0.28 ± 0.02) and Taylor White (0.29 ± 0.04) samples, and the Whangai Fm in Angora Road samples (0.36 ± 0.05) are non-radiogenic, and significantly lower than the present-day seawater $^{187}Os/^{188}Os$ value of ~ 1.02 to 1.06 (Woodhouse et al., 1999; Peucker-Ehrenbrink and Ravizza, 2000; Gannoun and Burton, 2014). The Os_i value (calculated at 58 Ma) for the one additional Waipawa Fm sample from Blacks Quarry in North Slope Basin ($\sim 0.24 \pm 0.01$; Table 2) is also non-radiogenic but lower than those of the Waipawa

Fm samples from the Orui-1A and Taylor White sections in the East Coast Basin (~0.28–0.29). If this sample represents a closed Re-Os system that has not been affected by post-depositional processes, then it would suggest that the Waipawa Fm in the North Slope Basin is either slightly younger or was deposited in a more open marine setting with less radiogenic Os_i . The latter appears more likely because the sample is from an allochthonous sequence that was emplaced from an everted marine basin with oceanic volcanic basement, at least 350 km north of its present location (Ballance and Spörli, 1979; Hollis et al., 2006). The Os_i values for the Waipawa Fm samples from the East Coast Basin are broadly similar to those of time correlative units from the central Pacific Ocean (0.26–0.33; Fig. 9a), suggesting that the basin was mixing with, at least, the wider Pacific Ocean. In addition, the observed Os_i values may be indicative of the global seawater $^{187}Os/^{188}Os$ values at the time given that paleo-ocean circulation patterns show that the Pacific, Atlantic and Indian oceans were all connected 59 Ma ago (Fig. 9a; Haq, 1981; Barron and Peterson, 1991; Thomas et al., 2003; Batenburg et al., 2018).

A composite record of $^{187}Os/^{188}Os$ values from sedimentary rocks spanning the period between 70 and 50 Ma and including the $^{187}Os/^{188}Os$ values for the Waipawa and Whangai formations in the present study (Fig. 9b), provides a broader temporal context in which the source of the non-radiogenic Os in the Paleocene can be examined. The $^{187}Os/^{188}Os$ value for the Waipawa Fm is based on the mean Os_i values [calculated at 59 Ma – the established biostratigraphic age (Hollis et al., 2014); Table 2] for the Orui-1A samples which, unlike the Taylor White samples, demonstrate an isochronous Re-Os relationship (Fig. 7). The obtained composite record highlights a progressive shift to low $^{187}Os/^{188}Os$ ratios from a value of ~0.61 in the latest Cretaceous (~68 Ma) to ~0.28 in late Paleocene (Fig. 9b). In particular, the

¹⁸⁷Os/¹⁸⁸Os value of ~0.28 at ca. 59 Ma during the deposition of the Waipawa Fm coincides with the minimum before the marine ¹⁸⁷Os/¹⁸⁸Os trend increases leading up to the Paleocene-Eocene boundary. Superimposed upon the overall decreasing trend in ¹⁸⁷Os/¹⁸⁸Os values from the latest Cretaceous to the late Paleocene is the abrupt negative excursion at ca. 66 Ma associated with the Cretaceous-Paleogene (K-Pg) impact event (Fig. 9b; Pegram and Turekian, 1999; Ravizza and VonderHaar, 2012). Extra-terrestrial impact events are distinguished in the marine Os record by abrupt shifts to low ¹⁸⁷Os/¹⁸⁸Os values (resulting from a sudden influx of non-radiogenic Os), followed by recovery to pre-impact values over a short duration of time (Paquay et al., 2008; Ravizza and VonderHaar, 2012). By contrast, the gradual nature of the long-term decline in ¹⁸⁷Os/¹⁸⁸Os values from the latest Cretaceous to late Paleocene indicates either a progressive increase in the supply of non-radiogenic Os or diminished supply of radiogenic Os from continental weathering.

A number of events have been proposed as potential sources of the non-radiogenic Os during this period. These include emplacement of large igneous provinces such as the Deccan Traps (Ravizza and Peucker-Ehrenbrink, 2003; Robinson et al., 2009) and the first eruptive phase of the North Atlantic Igneous Province (Peucker-Ehrenbrink and Ravizza, 2012), as well as weathering of exhumed large ophiolites such as the Papuan Ultramafic Belt (Fig. 9b; Lus et al., 2004; Peucker-Ehrenbrink and Ravizza, 2012). It is unclear, however, how much these events contributed to the ¹⁸⁷Os/¹⁸⁸Os decline given the significant time gaps between them and the long duration of the decline. Interestingly, though, the ¹⁸⁷Os/¹⁸⁸Os record is correlated with global temperature proxies ($\delta^{18}\text{O}$, TEX₈₆) and the carbon isotope ($\delta^{13}\text{C}$) record for much of the Paleocene and into the early Eocene (Figs 9b, 10). The temperature records indicate moderate cooling between 64 and 58 Ma followed by a more

pronounced warming trend (by ~10 °C) to around 53 Ma (Bijl et al., 2009; Hollis et al., 2012; Hollis et al., 2014; Westerhold et al., 2018). The temperature minimum at around 58.7 Ma coincides with the $^{187}\text{Os}/^{188}\text{Os}$ minimum and deposition of the Waipawa Fm (Fig. 10b, c). The simplest interpretation for these observations is that the gradual shift to low $^{187}\text{Os}/^{188}\text{Os}$ values in the middle–late Paleocene relates to a reduction in global rates of continental weathering as temperature (and thus, the hydrological cycle) decreased, whereas the positive shift from the late Paleocene to early Eocene relates to increased rates of continental weathering in response to rising temperatures and an accelerated hydrological cycle (Zachos et al., 2008). This interpretation, although based on an assumption that fluxes of non-radiogenic Os to the ocean remain relatively constant during this period, is supported by previous findings that attributed the positive excursion in the $^{187}\text{Os}/^{188}\text{Os}$ ratios at the Paleocene-Eocene Thermal Maximum (PETM) to increased chemical weathering from an accelerated hydrological cycle, albeit on a much shorter time scale and a more severe climatic perturbation (Ravizza et al., 2001; Wieczorek et al., 2013; Dickson et al., 2015).

The $\delta^{13}\text{C}$ record follows a similar trend to those of the $\delta^{18}\text{O}$ and TEX_{86} records, but with a maximum at around 58 Ma, ~1 my later than the temperature and $^{187}\text{Os}/^{188}\text{Os}$ minimum (Fig. 10a). Temporal variations in the stable carbon isotope composition have been attributed to many factors, the discussion of which is beyond the scope of this paper. However, the broad correlation of $^{187}\text{Os}/^{188}\text{Os}$ with $\delta^{13}\text{C}$ is consistent with the inference that continental weathering patterns may have contributed significantly to the observed middle Paleocene to early Eocene $^{187}\text{Os}/^{188}\text{Os}$ record. This is because enhanced weathering of isotopically evolved (ancient) organic-rich rocks would have driven the seawater $^{187}\text{Os}/^{188}\text{Os}$ ratios to more radiogenic values and

shifted the carbon isotope composition to lighter values (Ravizza and Esser, 1993). This explanation, however, requires that there was an exposure of large amounts of significantly older organic-rich rocks. It has been suggested that large quantities of neo-Tethyan (Triassic to Cretaceous) marine sediments were exhumed, oxidised and eroded during the initial stages of Indian-Asian collision causing the late Paleocene to early Eocene shift to lighter $\delta^{13}\text{C}$ values and the coeval global warming via the greenhouse effect (Beck et al., 1995). Using an estimated average $^{187}\text{Re}/^{188}\text{Os}$ value of 517 for organic-rich shales (bootstrapped 95% confidence interval of 468 to 582; calculated from a geochemical database of organic-rich sediments from 42 different sources; Dubin and Peucker-Ehrenbrink, 2015) and seawater $^{187}\text{Os}/^{188}\text{Os}$ values ranging from ~0.2 to 0.9 for the Triassic to Cretaceous period (100–250 Ma; Cohen and Coe, 2007; Porter et al., 2013; Dubin and Peucker-Ehrenbrink, 2015; Them et al., 2017; van Acken et al., 2019), these exhumed marine sediments would have contained $^{187}\text{Os}/^{188}\text{Os}$ values ranging from 1.1 to 3.1, with an average of 2.1, significantly more radiogenic than the average $^{187}\text{Os}/^{188}\text{Os}$ value of 1.4 for the upper continental crust. Further, the high abundance of Re and Os in organic-rich sediments coupled with the propensity of the Os hosted in these sediments to be readily mobilized during chemical weathering compared to the Os in typical granitic upper continental crust (Peucker-Ehrenbrink and Hannigan, 2000; Jaffe et al., 2002; Pierson-Wickmann et al., 2002; Georgiev et al., 2012; Dubin and Peucker-Ehrenbrink, 2015) supports the interpretation that exposure of the neo-Tethyan organic-rich sediments in the late Paleocene may have had potential to disproportionately drive seawater $^{187}\text{Os}/^{188}\text{Os}$ to more radiogenic values.

5. Conclusions

The Re-Os geochronology of the Waipawa Fm has yielded ages of 57.5 ± 3.5 Ma from the Orui-1A drill hole and 58.3 ± 6.5 Ma from the Taylor White section that are in close agreement with the available biostratigraphic age range for the formation (59.4 to 58.7 Ma; Hollis et al., 2014). These are the first radiometric ages for this formation and demonstrate the potential of the Re-Os method for future dating of correlative units identified in other sedimentary basins across the Southwest Pacific. However, the large uncertainties in the Re-Os dates make it difficult to refine the age control and establish whether all known occurrences of the Waipawa Fm are coeval. Future Re-Os studies on the formation should target intervals where the spread in Re-Os ratios is likely to be larger based on variation in organic matter type and other geochemical features, especially in the upper part of the formation. The results from the Taylor White section also highlight the benefit of using fresh core material for such work given the apparent high susceptibility of the Waipawa Fm to oxidative weathering that may disturb the Re-Os system.

The initial $^{187}\text{Os}/^{188}\text{Os}$ values for the Waipawa (~ 0.28) and Whangai (~ 0.36) formations are non-radiogenic and broadly similar to $^{187}\text{Os}/^{188}\text{Os}$ values from coeval pelagic sediments, further constraining the low-resolution marine Os record for the Paleocene. The broad correlation between the $^{187}\text{Os}/^{188}\text{Os}$ record and the global temperature proxies ($\delta^{18}\text{O}$, TEX_{86}) and carbon isotope ($\delta^{13}\text{C}$) records from the middle Paleocene to early Eocene suggests that changes in global weathering patterns may have been the main driver of the Os geochemical cycle during this time.

Acknowledgements

This project and the PhD scholarship awarded to EKR were funded by the Ministry of Business, Innovation and Employment (MBIE), New Zealand, as part of the GNS Science-led programme “Understanding petroleum source rocks, fluids, and plumbing systems in New Zealand basins: a critical basis for future oil and gas discoveries” (Contract C05X1507). DS acknowledges the Total Endowment Fund and CUG Wuhan Dida Scholarship. We thank D. van Acken and an anonymous reviewer for their insightful comments and suggestions, and B. Kamber for effective editorial handling. We also thank Antonia Hoffman, Geoff Nowell, Bruce Charlier and Luisa Ashworth for their technical assistance, and CRL Energy Ltd for the sulfur analyses. Hannu Seebeck is thanked for providing the global paleogeographic map.

Figure captions

Fig. 1. a) Map of the study area showing sample locations and distribution of Waipawa organofacies in the Southwest Pacific. Geological data extracted from QMAP 1:250K data set (Heron, 2014). Abbreviations: R-NB = Reinga-Northland Basin; NSB = North Slope Basin; DTB = Deepwater Taranaki Basin; TB = Taranaki Basin; ECB = East Coast Basin; WCB = West Coast Basin; CB = Canterbury Basin; GSB = Great South Basin. b) Paleogeographic reconstruction of the New Zealand region in the late Paleocene (58 Ma), adapted after King (2000), Killops et al. (2000) and Hollis et al. (2014).

Fig. 2. Chronostratigraphic column of the East Coast Basin from the Late Cretaceous to early Eocene (after King, 2000; Hollis et al., 2014). Nannofossil assemblages are correlated to the biostratigraphic zonation scheme of Martini (1971), with absolute ages for events from Gradstein et al. (2012). Calcareous nannofossils zonation (CNZ) after Crouch et al. (2014). IUGS = International Union of Geological Sciences; UCM = Upper Calcareous Member.

Fig. 3. Cross-plots of bulk pyrolysis data identifying the type and maturity of organic matter present in the Waipawa and Whangai formations. a) TOC vs HI, with the oil- (1) and gas-prone (2) trends of Naeher et al. (2019). b) OI vs T_{max} . c) Modified van Krevelen diagram showing the general maturation pathways for the main types of organic matter (after Hunt, 1995).

Fig. 4. Cross-plots of TOC vs Re (a) and ^{192}Os (b) concentrations in the Waipawa and Whangai formations. Separate trendlines and correlation coefficients are shown by locality. Outlier samples TW-17 and TW-29 (unfilled red squares) are excluded from the trendlines (see text for discussion).

Fig. 5. Cross-plots of total sulfur vs a) Re concentrations, b) ^{192}Os concentrations and c) $^{187}\text{Re}/^{188}\text{Os}$ for the Waipawa and Whangai formations samples. Outlier samples TW-17 and TW-29 are excluded from these plots.

Fig. 6. Cross-plots of normalised forms of sulfur and Re and ^{192}Os concentrations. Organic sulfur ($S_{\text{org}}/S_{\text{tot}}$) vs Re (a) and ^{192}Os (b); pyritic sulfur ($S_{\text{pyr}}/S_{\text{tot}}$) vs Re (c) and ^{192}Os (d); sulphate sulfur ($S_{\text{sul}}/S_{\text{tot}}$) vs Re (e) and ^{192}Os (f). Outlier samples TW-17 and TW-29 are excluded from these plots. The legend shown in Fig. 6f is used for all plots.

Fig. 7. Re-Os geochronological results for the Waipawa Fm samples from Orui-1A core. All samples are plotted in (a) and (b) whereas sample Orui-11e is excluded in (c) and (d). Regression of the Re-Os isotope data together with the 2σ uncertainties in the isotope ratios and the associated error correlation functions (ρ) were done using the beta version of Isochron program (Li et al., 2019), which incorporates the Isoplot algorithm (a and c) (Ludwig, 2012) and the Monte Carlo method (b and d). The Re-Os dates and Os_i composition are very similar in both methods, except that the uncertainties from the Monte Carlo method are higher, especially for the Model 1 scenario of the Isoplot program (c) (Li et al., 2019). See text for discussion. The bracketed age uncertainty includes the uncertainty in the ^{187}Re decay constant (λ), where $\lambda = 1.666 \pm 0.0031 \times 10^{-11} \text{ yr}^{-1}$ (Smoliar et al., 1996; Selby et al., 2007).

Fig. 8. Re-Os geochronological results for the Waipawa Fm samples from the Taylor White section (a and b) and Whangai Fm samples from the Angora Road section (c and d). The data were regressed using the beta version of the Isochron program (Li et al., 2019) as described in Fig. 7 and in the text. Outlier samples TW-17 and TW-29 are not included in the regression. Note that the uncertainties from the Monte Carlo method are lower than those of the Model 3 scenario of the Isoplot method. See text

for discussion. The bracketed age uncertainty includes the uncertainty in the ^{187}Re decay constant (λ), where $\lambda = 1.666 \pm 0.0031 \times 10^{-11} \text{ yr}^{-1}$ (Smoliar et al., 1996; Selby et al., 2007).

Fig. 9. a) A GPlates global paleogeographic reconstruction of the late Paleocene (59 Ma) using the relative finite rotations, continental polygons and coastlines from Matthews et al. (2016), placed in the global paleomagnetic reference frame of Torsvik et al. (2012). Ocean circulation patterns are inferred from Haq (1981), Barron and Peterson (1991), Thomas et al. (2003) and Batenburg et al. (2018). b) composite $^{187}\text{Os}/^{188}\text{Os}$ record of the latest Cretaceous to early Eocene period (70–50 Ma). The $^{187}\text{Os}/^{188}\text{Os}$ value for the Waipawa Fm is based on mean Os_i ratios (calculated at 59 Ma) from Orui-1A samples (see text for discussion) whereas that of the Whangai Fm is derived from the Angora Road samples isochron. The benthic foraminiferal oxygen isotope ($\delta^{18}\text{O}$) record from ODP site 1209 is shown for the period between 66 and 50 Ma (Westerhold et al., 2017; 2018). Os isotope data sources: LL44-GPC3 = Pegram and Turekian (1999); DSDP 549 = Ravizza et al. (2001); CD29-2 = Klemm et al. (2005); ODP 886C = Ravizza (2007); ODP 690C and ODP 1262B = Ravizza and VonderHaar (2012) and ODP 865 = Rolewicz (2013). Not shown are initial $^{187}\text{Os}/^{188}\text{Os}$ ratios for late Maastrichtian (65.5 to 68.5 Ma) sediments from ODP 690, DSDP 577 and DSDP 525 (Robinson et al., 2009) that agree well with the data from Ravizza (2007) and Ravizza and VonderHaar (2012). NAIP = North Atlantic Igneous Province; Papuan UMB = Papuan Ultramafic Belt; PETM = Paleocene-Eocene Thermal Maximum.

Fig. 10. Trends in benthic stable carbon isotope values ($\delta^{13}\text{C}$) (a), benthic oxygen isotope values ($\delta^{18}\text{O}$) (b) and TEX_{86} values (c), overlain by a smoothing of the composite $^{187}\text{Os}/^{188}\text{Os}$ data from Fig. 9 (brown line). Data were smoothed using Origin Pro 2018 v9.5.1 software, employing the 5-point adjacent averaging method. TEX_{86} data are from Hollis et al. (2014); benthic foraminiferal $\delta^{18}\text{O}$ and $\delta^{13}\text{C}$ records are from ODP sites 1209, 1262 and 1263 (Westerhold et al., 2017, 2018), calibrated to the age model of Westerhold et al. (2017). The $^{187}\text{Os}/^{188}\text{Os}$ data points for Waipawa and Whangai formations are shown by the purple and blue squares, respectively, with the legends shown applying to all plots.

References

- Ballance, P.F., Spörli, K.B., 1979. Northland Allochthon. *Journal of the Royal Society of New Zealand*, 9: 259–275.
- Barnet, J.S.K., Littler, K., Westerhold, T., Kroon, D., Leng, M.J., Bailey, I., Röhl, U., Zachos, J.C., 2019. A High-Fidelity Benthic Stable Isotope Record of Late Cretaceous–Early Eocene Climate Change and Carbon-Cycling. *Paleoceanography and Paleoclimatology*, 34: 672–691.
- Barron, E.J., Peterson, W.H., 1991. The Cenozoic ocean circulation based on ocean General Circulation Model results. *Palaeogeography, Palaeoclimatology, Palaeoecology*, 83: 1–28.
- Batenburg, S.J., Voigt, S., Friedrich, O., Osborne, A.H., Bornemann, A., Klein, T., Pérez-Díaz, L., Frank, M., 2018. Major intensification of Atlantic overturning circulation at the onset of Paleogene greenhouse warmth. *Nature Communications*, 9: 4954.
- Beck, R.A., Burbank, D.W., Sercombe, W.J., Olson, T.L., Khan, A.M., 1995. Organic carbon exhumation and global warming during the early Himalayan collision. *Geology*, 23: 387–390.
- Bertoni, M.E., Rooney, A.D., Selby, D., Alkmim, F.F., Le Heron, D.P., 2014. Neoproterozoic Re-Os systematics of organic-rich rocks in the São Francisco Basin, Brazil and implications for hydrocarbon exploration. *Precambrian Research*, 255: 355–366.
- Bijl, P.K., Schouten, S., Sluijs, A., Reichert, G.-J., Zachos, J.C., Brinkhuis, H., 2009. Early Palaeogene temperature evolution of the southwest Pacific Ocean. *Nature*, 461: 776.
- Bland, K.J., Strogen, D.P., Morgans, H.E.G., Ventura, G.T., 2014. Record of section descriptions and sample collection from the Tahuokaretu and Taylor White

- sections, southern Hawke's Bay, 1–3 May 2014, for micropaleontological and source rock analyses. GNS Science internal report 2014/03, 55 pp.
- Burton, K.W., Bourdon, B., Birck, J.-L., Allègre, C.J., Hein, J.R., 1999. Osmium isotope variations in the oceans recorded by Fe–Mn crusts. *Earth and Planetary Science Letters*, 171: 185–197.
- Cohen, A.S., 2004. The rhenium-osmium isotope system: applications to geochronological and palaeoenvironmental problems. *Journal of the Geological Society*, 161: 729–734.
- Cohen, A.S., Coe, A.L., 2007. The impact of the Central Atlantic Magmatic Province on climate and on the Sr- and Os-isotope evolution of seawater. *Palaeogeography, Palaeoclimatology, Palaeoecology*, 244: 374–390.
- Cohen, A.S., Coe, A.L., Bartlett, J.M., Hawkesworth, C.J., 1999. Precise Re-Os ages of organic-rich mudrocks and the Os isotope composition of Jurassic seawater. *Earth and Planetary Science Letters*, 167: 159–173.
- Colodner, D., Sachs, J., Ravizza, G., Turekian, K.K., Edmond, J., Boyle, E., 1993. The geochemical cycle of rhenium: a reconnaissance. *Earth and Planetary Science Letters*, 117: 205–221.
- Corfield, R.M., Cartlidge, J.E., 1992. Oceanographic and climatic implications of the Palaeocene carbon isotope maximum. *Terra Nova*, 4: 443–455.
- Creaser, R., Szatmari, P., Milani, E.J., 2008. Extending Re-Os shale geochronology to lacustrine depositional systems: a case study from the major hydrocarbon source rocks of the Brazilian Mesozoic marginal basins. *Proceedings of the 33rd International Geological Congress, Oslo*.
- Creaser, R.A., Sannigrahi, P., Chacko, T., Selby, D., 2002. Further evaluation of the Re-Os geochronometer in organic-rich sedimentary rocks: a test of hydrocarbon maturation effects in the Exshaw Formation, Western Canada Sedimentary Basin. *Geochimica et Cosmochimica Acta*, 66: 3441–3452.
- Crouch, E.M., Willumsen, P.S., Kulhanek, D.K., Gibbs, S.J., 2014. A revised Paleocene (Teurian) dinoflagellate cyst zonation from eastern New Zealand. *Review of Palaeobotany and Palynology*, 202: 47–79.
- Crusius, J., Calvert, S., Pedersen, T., Sage, D., 1996. Rhenium and molybdenum enrichments in sediments as indicators of oxic, suboxic and sulfidic conditions of deposition. *Earth and Planetary Science Letters*, 145: 65–78.
- Crusius, J., Thomson, J., 2000. Comparative behavior of authigenic Re, U, and Mo during reoxidation and subsequent long-term burial in marine sediments. *Geochimica et Cosmochimica Acta*, 64: 2233–2242.
- Cumming, V.M., Selby, D., Lillis, P.G., 2012. Re-Os geochronology of the lacustrine Green River Formation: Insights into direct depositional dating of lacustrine successions, Re-Os systematics and paleocontinental weathering. *Earth and Planetary Science Letters*, 359–360: 194–205.
- De Lena, L.F., Taylor, D., Guex, J., Bartolini, A., Adatte, T., van Acken, D., Spangenberg, J.E., Samankassou, E., Vennemann, T., Schaltegger, U., 2019. The driving mechanisms of the carbon cycle perturbations in the late Pliensbachian (Early Jurassic). *Scientific Reports*, 9: 18430.
- Dickson, A.J., Cohen, A.S., Coe, A.L., Davies, M., Shcherbinina, E.A., Gavrilov, Y.O., 2015. Evidence for weathering and volcanism during the PETM from Arctic Ocean and Peri-Tethys osmium isotope records. *Palaeogeography, Palaeoclimatology, Palaeoecology*, 438: 300–307.

- Didyk, B.M., Simoneit, B.R.T., Brassell, S.C., Eglinton, G., 1978. Organic geochemical indicators of palaeoenvironmental conditions of sedimentation. *Nature*, 272: 216–222.
- Du Vivier, A.D.C., Selby, D., Condon, D.J., Takashima, R., Nishi, H., 2015. Pacific $^{187}\text{Os}/^{188}\text{Os}$ isotope chemistry and U-Pb geochronology: Synchronicity of global Os isotope change across OAE 2. *Earth and Planetary Science Letters*, 428: 204–216.
- Du Vivier, A.D.C., Selby, D., Sageman, B.B., Jarvis, I., Gröcke, D.R., Voigt, S., 2014. Marine $^{187}\text{Os}/^{188}\text{Os}$ isotope stratigraphy reveals the interaction of volcanism and ocean circulation during Oceanic Anoxic Event 2. *Earth and Planetary Science Letters*, 389: 23–33.
- Dubin, A., Peucker-Ehrenbrink, B., 2015. The importance of organic-rich shales to the geochemical cycles of rhenium and osmium. *Chemical Geology*, 403: 111–120.
- Esser, B.K., Turekian, K.K., 1993. The osmium isotopic composition of the continental crust. *Geochimica et Cosmochimica Acta*, 57: 3093–3104.
- Field, B.D., Naeher, S., Clowes, C.D., Shepherd, C.L., Hollis, C.J., Sykes, R., Ventura, G.T., Pascher, K.M., Griffin, A.G., 2018. Depositional influences on the petroleum potential of the Waipawa Formation in the Orui-1A drillhole, Wairarapa. GNS Science report 2017/49, 75 pp.
- Field, B.D., Uruski, C.I., Beu, A.G., Browne, G.H., Crampton, J.S., Funnell, R.H., Killops, S.D., Laird, M., Mazengarb, C., Morgans, H.E.G., Rait, G.J., Smale, D., Strong, C.P., 1997. Cretaceous–Cenozoic geology and petroleum systems of the East Coast region, New Zealand, Monograph 19, 7 enclosures. Institute of Geological & Nuclear Sciences Limited, Lower Hutt, New Zealand, 301 pp.
- Finlay, A.J., Selby, D., Gröcke, D.R., 2010. Tracking the Hirnantian glaciation using Os isotopes. *Earth and Planetary Science Letters*, 293: 339–348.
- Gannoun, A., Burton, K.W., 2014. High precision osmium elemental and isotope measurements of North Atlantic seawater. *Journal of Analytical Atomic Spectrometry*, 29: 2330–2342.
- Georgiev, S., Stein, H.J., Hannah, J.L., Bingen, B., Weiss, H.M., Piasecki, S., 2011. Hot acidic Late Permian seas stifle life in record time. *Earth and Planetary Science Letters*, 310: 389–400.
- Georgiev, S., Stein, H.J., Hannah, J.L., Weiss, H.M., Bingen, B., Xu, G., Rein, E., Hatl, V., Lseth, H., Nali, M., Piasecki, S., 2012. Chemical signals for oxidative weathering predict Re-Os isochroneity in black shales, East Greenland. *Chemical Geology*, 324–325: 108–121.
- Georgiev, S.V., Stein, H.J., Hannah, J.L., Xu, G., Bingen, B., Weiss, H.M., 2017. Timing, duration, and causes for Late Jurassic–Early Cretaceous anoxia in the Barents Sea. *Earth and Planetary Science Letters*, 461: 151–162.
- Gradstein, F.M., Ogg, J.G., Schmitz, M., Ogg, G., 2012. *The Geologic Time Scale 2012*, 2. Elsevier.
- Gramlich, J.W., Murphy, T.J., Garner, E.L., Shields, W.R., 1973. Absolute isotopic abundance ratio and atomic weight of a reference sample of rhenium. *Journal of Research of the National Bureau of Standards A*, 77A: 691–698.
- Haq, B.U., 1981. Paleogene Paleooceanography: Early Cenozoic Oceans Revisited. *Oceanologica Acta*, Special issue (0399-1784).
- Harris, N.B., Mnich, C.A., Selby, D., Korn, D., 2013. Minor and trace element and Re-Os chemistry of the Upper Devonian Woodford Shale, Permian Basin, west

- 938 Texas: Insights into metal abundance and basin processes. *Chemical*
939 *Geology*, 356: 76–93.
- 940 Heron, D.W., (custodian), 2014. Geological map of New Zealand 1:250,000. GNS
941 Science geological map 1. GNS Science Lower Hutt, New Zealand. 1 CD.
- 942 Hines, B.R., Gazley, M.F., Collins, K.S., Bland, K.J., Crampton, J.S., Ventura, G.T.,
943 2019. Chemostratigraphic resolution of widespread reducing conditions in the
944 southwest Pacific Ocean during the Late Paleocene. *Chemical Geology*, 504:
945 236–252.
- 946 Hollis, C.J., Field, B.D., Crouch, E.M., Sykes, R., 2006. How good a source rock is
947 the Waipawa (black shale) Formation beyond the East Coast Basin? An
948 outcrop-based case study from Northland. 2006 New Zealand Petroleum
949 Conference Proceedings, Auckland, New Zealand, 8 pp.
- 950 Hollis, C.J., Tayler, M.J.S., Andrew, B., Taylor, K.W., Lurcock, P., Bijl, P.K.,
951 Kulhanek, D.K., Crouch, E.M., Nelson, C.S., Pancost, R.D., Huber, M., Wilson,
952 G.S., Ventura, G.T., Crampton, J.S., Schiøler, P., Phillips, A., 2014. Organic-
953 rich sedimentation in the South Pacific Ocean associated with Late Paleocene
954 climatic cooling. *Earth-Science Reviews*, 134: 81–97.
- 955 Hollis, C.J., Taylor, K.W.R., Handley, L., Pancost, R.D., Huber, M., Creech, J.B.,
956 Hines, B.R., Crouch, E.M., Morgans, H.E.G., Crampton, J.S., Gibbs, S.,
957 Pearson, P.N., Zachos, J.C., 2012. Early Paleogene temperature history of the
958 Southwest Pacific Ocean: Reconciling proxies and models. *Earth and*
959 *Planetary Science Letters*, 349–350: 53–66.
- 960 Hunt, J.M., 1995. *Petroleum Geochemistry and Geology*. W. H. Freeman and
961 Company, New York, 743 pp.
- 962 Ingall, E.D., Cappellen, P.V., 1990. Relation between sedimentation rate and burial of
963 organic phosphorus and organic carbon in marine sediments. *Geochimica et*
964 *Cosmochimica Acta*, 54: 373–386.
- 965 Jaffe, L.A., Peucker-Ehrenbrink, B., Petsch, S.T., 2002. Mobility of rhenium, platinum
966 group elements and organic carbon during black shale weathering. *Earth and*
967 *Planetary Science Letters*, 198: 339–353.
- 968 Jones, M.M., Ibarra, D.E., Gao, Y., Sageman, B.B., Selby, D., Chamberlain, C.P.,
969 Graham, S.A., 2018. Evaluating Late Cretaceous OAEs and the influence of
970 marine incursions on organic carbon burial in an expansive East Asian paleo-
971 lake. *Earth and Planetary Science Letters*, 484: 41–52.
- 972 Kendall, B., Creaser, R.A., Gordon, G.W., Anbar, A.D., 2009a. Re-Os and Mo
973 isotope systematics of black shales from the Middle Proterozoic Velkerri and
974 Wollongorang Formations, McArthur Basin, northern Australia. *Geochimica et*
975 *Cosmochimica Acta*, 73: 2534–2558.
- 976 Kendall, B., Creaser, R.A., Selby, D., 2006. Re-Os geochronology of postglacial
977 black shales in Australia: Constraints on the timing of “Sturtian” glaciation.
978 *Geology*, 34: 729–732.
- 979 Kendall, B., Creaser, R.A., Selby, D., 2009b. ^{187}Re - ^{187}Os geochronology of
980 Precambrian organic-rich sedimentary rocks. The Geological Society, London,
981 Special Publications, 326: 85–107.
- 982 Kendall, B.S., Creaser, R.A., Ross, G.M., Selby, D., 2004. Constraints on the timing
983 of Marinoan “Snowball Earth” glaciation by ^{187}Re - ^{187}Os dating of a
984 Neoproterozoic, post-glacial black shale in Western Canada. *Earth and*
985 *Planetary Science Letters*, 222: 729–740.

- Killops, S.D., Cook, R.A., Sykes, R., Boudou, J.P., 1997. Petroleum potential and oil-source correlation in the Great South and Canterbury Basins. *New Zealand Journal of Geology and Geophysics*, 40: 405–423.
- Killops, S.D., Hollis, C.J., Morgans, H.E.G., Sutherland, R., Field, B.D., Leckie, D.A., 2000. Paleoceanographic significance of Late Paleocene dysaerobia at the shelf/slope break around New Zealand. *Palaeogeography, Palaeoclimatology, Palaeoecology*, 156: 51–70.
- King, P.R., 2000. New Zealand's changing configuration in the last 100 million years; plate tectonics, basin development, and depositional setting. 2000 New Zealand Petroleum Conference Proceedings, Crown Minerals, Ministry of Commerce Wellington, New Zealand, 131–145 pp.
- Klemm, V., Levasseur, S., Frank, M., Hein, J.R., Halliday, A.N., 2005. Osmium isotope stratigraphy of a marine ferromanganese crust. *Earth and Planetary Science Letters*, 238: 42–48.
- Kulhanek, D., Crouch, E., J. S. Tayler, M., Hollis, C., 2015. Paleocene calcareous nannofossils from East Coast, New Zealand: biostratigraphy and palaeoecology. *Journal of Nannoplankton Research*, 35: 155–176.
- Kurtz, A.C., Kump, L.R., Arthur, M.A., Zachos, J.C., Paytan, A., 2003. Early Cenozoic decoupling of the global carbon and sulfur cycles. *Paleoceanography*, 18: 1090.
- Langrock, U., Stein, R., 2004. Origin of marine petroleum source rocks from the Late Jurassic to Early Cretaceous Norwegian Greenland Seaway—evidence for stagnation and upwelling. *Marine and Petroleum Geology*, 21: 157–176.
- Lewan, M.D., Maynard, J.B., 1982. Factors controlling enrichment of vanadium and nickel in the bitumen of organic sedimentary rocks. *Geochimica et Cosmochimica Acta*, 46: 2547–2560.
- Li, Y., Zhang, S., Hobbs, R., Caiado, C., Sproson, A.D., Selby, D., Rooney, A.D., 2019. Monte Carlo sampling for error propagation in linear regression and applications in isochron geochronology. *Science Bulletin*, 64: 189–197.
- Littler, K., Röhl, U., Westerhold, T., Zachos, J.C., 2014. A high-resolution benthic stable-isotope record for the South Atlantic: Implications for orbital-scale changes in Late Paleocene–Early Eocene climate and carbon cycling. *Earth and Planetary Science Letters*, 401: 18–30.
- Liu, J., Pearson, D.G., 2014. Rapid, precise and accurate Os isotope ratio measurements of nanogram to sub-nanogram amounts using multiple Faraday collectors and amplifiers equipped with 10¹² Ω resistors by N-TIMS. *Chemical Geology*, 363: 301–311.
- Liu, J., Selby, D., 2018. A matrix-matched reference material for validating petroleum Re-Os measurements. *Geostandards and Geoanalytical Research*, 42: 97–113.
- Ludwig, K.R., 1980. Calculation of uncertainties of U-Pb isotope data. *Earth and Planetary Science Letters*, 46: 212–220.
- Ludwig, K.R., 2012. Isoplot, version 3.75: A geochronological Toolkit for Microsoft Excel. Berkeley Geochronology Center Special Publication No. 5.
- Lus, W.Y., McDougall, I., Davies, H.L., 2004. Age of the metamorphic sole of the Papuan Ultramafic Belt ophiolite, Papua New Guinea. *Tectonophysics*, 392: 85–101.
- Martini, E., 1971. Standard Tertiary and Quaternary calcareous nannoplankton zonation. In: Farinacci, A.E. (Editor), *Proceedings of the Second Planktonic Conference Roma*, Edizioni Tecnoscienza, Rome, pp. 739–785.

- Matthews, K.J., Maloney, K.T., Zahirovic, S., Williams, S.E., Seton, M., Müller, R.D., 2016. Global plate boundary evolution and kinematics since the late Paleozoic. *Global and Planetary Change*, 146: 226–250.
- McArthur, J.M., Algeo, T.J., van de Schootbrugge, B., Li, Q., Howarth, R.J., 2008. Basinal restriction, black shales, Re-Os dating, and the Early Toarcian (Jurassic) oceanic anoxic event. *Paleoceanography*, 23.
- Moore, P.R., 1988. Stratigraphy, composition, and environment of deposition of the Whangai Formation and associated Late Cretaceous-Paleocene rocks, eastern North Island, New Zealand. *New Zealand Geological Survey Bulletin*, 100: 82.
- Moore, P.R., 1989. Stratigraphy of the Waipawa Black Shale (Paleocene), eastern North Island, New Zealand. *New Zealand Geological Survey record*, 38, 19 pp.
- Morford, J.L., Emerson, S., 1999. The geochemistry of redox sensitive trace metals in sediments. *Geochimica et Cosmochimica Acta*, 63: 1735–1750.
- Naeher, S., Hollis, C.J., Clowes, C.D., Ventura, G.T., Shepherd, C.L., Crouch, E.M., Morgans, H.E.G., Bland, K.J., Strogon, D.P., Sykes, R., 2019. Depositional and organofacies influences on the petroleum potential of an unusual marine source rock: Waipawa Formation (Paleocene) in southern East Coast Basin, New Zealand. *Marine and Petroleum Geology*, 104: 468–488.
- Nowell, G.M., Luguet, A., Pearson, D.G., Horstwood, M.S.A., 2008. Precise and accurate $^{186}\text{Os}/^{188}\text{Os}$ and $^{187}\text{Os}/^{188}\text{Os}$ measurements by multi-collector plasma ionisation mass spectrometry (MC-ICP-MS) part I: Solution analyses. *Chemical Geology*, 248: 363–393.
- Owensworth, E., Selby, D., Ottley, C.J., Unsworth, E., Raab, A., Feldmann, J., Sproson, A.D., Kuroda, J., Faidutti, C., Bucker, P., 2019. Tracing the natural and anthropogenic influence on the trace elemental chemistry of estuarine macroalgae and the implications for human consumption. *Science of The Total Environment*, 685: 259–272.
- Paquay, F.S., Ravizza, G.E., Dalai, T.K., Peucker-Ehrenbrink, B., 2008. Determining chondritic impactor size from the marine osmium isotope record. *Science*, 320: 214.
- Pegram, W.J., Turekian, K.K., 1999. The osmium isotopic composition change of Cenozoic sea water as inferred from a deep-sea core corrected for meteoritic contributions. *Geochimica et Cosmochimica Acta*, 63: 4053–4058.
- Percival, L.M.E., Cohen, A.S., Davies, M.K., Dickson, A.J., Hesselbo, S.P., Jenkyns, H.C., Leng, M.J., Mather, T.A., Storm, M.S., Xu, W., 2016. Osmium isotope evidence for two pulses of increased continental weathering linked to Early Jurassic volcanism and climate change. *Geology*, 44: 759–762.
- Peucker-Ehrenbrink, B., Hannigan, R.E., 2000. Effects of black shale weathering on the mobility of rhenium and platinum group elements. *Geology*, 28: 475–478.
- Peucker-Ehrenbrink, B., Ravizza, G., 2012. Chapter 8 - Osmium Isotope Stratigraphy. In: Gradstein, F.M., Ogg, J.G., Schmitz, M.D., Ogg, G.M. (Eds.), *The Geologic Time Scale*. Elsevier, Boston, pp. 145–166.
- Peucker-Ehrenbrink, B., Ravizza, G., 2000. The marine osmium isotope record. *Terra Nova*, 12: 205–219.
- Pierson-Wickmann, A.-C., Reisberg, L., France-Lanord, C., 2002. Behavior of Re and Os during low-temperature alteration: Results from Himalayan soils and altered black shales. *Geochimica et Cosmochimica Acta*, 66: 1539–1548.

- Poirier, A., Hillaire-Marcel, C., 2011. Improved Os-isotope stratigraphy of the Arctic Ocean. *Geophysical Research Letters*, 38: L14607.
- Porter, S.J., Selby, D., Suzuki, K., Gröcke, D., 2013. Opening of a trans-Pangaeian marine corridor during the Early Jurassic: Insights from osmium isotopes across the Sinemurian–Pliensbachian GSSP, Robin Hood's Bay, UK. *Palaeogeography, Palaeoclimatology, Palaeoecology*, 375: 50–58.
- Racionero-Gómez, B., Sproson, A.D., Selby, D., Gannoun, A., Gröcke, D.R., Greenwell, H.C., Burton, K.W., 2017. Osmium uptake, distribution, and $^{187}\text{Os}/^{188}\text{Os}$ and $^{187}\text{Re}/^{188}\text{Os}$ compositions in Phaeophyceae macroalgae, *Fucus vesiculosus*: Implications for determining the $^{187}\text{Os}/^{188}\text{Os}$ composition of seawater. *Geochimica et Cosmochimica Acta*, 199: 48–57.
- Racionero-Gómez, B., Sproson, A.D., Selby, D., Gröcke, D.R., Redden, H., Greenwell, H.C., 2016. Rhenium uptake and distribution in phaeophyceae macroalgae, *Fucus vesiculosus*. *Royal Society Open Science*, 3: 160161.
- Ravizza, G., 1993. Variations of the $^{187}\text{Os}/^{186}\text{Os}$ ratio of seawater over the past 28 million years as inferred from metalliferous carbonates. *Earth and Planetary Science Letters*, 118: 335–348.
- Ravizza, G., 2007. Reconstructing the marine $^{187}\text{Os}/^{188}\text{Os}$ record and the particulate flux of meteoritic osmium during the late Cretaceous. *Geochimica et Cosmochimica Acta*, 71: 1355–1369.
- Ravizza, G., Esser, B.K., 1993. A possible link between the seawater osmium isotope record and weathering of ancient sedimentary organic matter. *Chemical Geology*, 107: 255–258.
- Ravizza, G., Norris, R.N., Blusztajn, J., Aubry, M.P., 2001. An osmium isotope excursion associated with the Late Paleocene thermal maximum: Evidence of intensified chemical weathering. *Paleoceanography and Paleoclimatology* 16: 133–234.
- Ravizza, G., Peucker-Ehrenbrink, B., 2003. Chemostratigraphic evidence of Deccan volcanism from the marine osmium isotope record. *Science* 302: 1392–1395.
- Ravizza, G., Turekian, K.K., 1989. Application of the ^{187}Re - ^{187}Os system to black shale geochronometry. *Geochimica et Cosmochimica Acta*, 53: 3257–3262.
- Ravizza, G., VonderHaar, D., 2012. A geochemical clock in earliest Paleogene pelagic carbonates based on the impact-induced Os isotope excursion at the Cretaceous-Paleogene boundary. *Paleoceanography*, 27: PA3219.
- Robinson, N., Ravizza, G., Coccioni, R., Peucker-Ehrenbrink, B., Norris, R.N., 2009. A high-resolution marine $^{187}\text{Os}/^{188}\text{Os}$ record for the late Maastrichtian: Distinguishing the chemical fingerprints of Deccan volcanism and the KP impact event. *Earth and Planetary Science Letters*, 281: 159–168.
- Rolewicz, Z.L., 2013. Seawater Osmium Isotope Records from Pacific ODP and IODP Sites - Refining the Paleogene Curve and Dating Red Clay Sequences. Undergraduate research scholars Thesis, Texas A&M University.
- Rooney, A.D., Austermann, J., Smith, E.F., Li, Y., Selby, D., Dehler, C.M., Schmitz, M.D., Karlstrom, K.E., Macdonald, F.A., 2017. Coupled Re-Os and U-Pb geochronology of the Tonian Chuar Group, Grand Canyon. *GSA Bulletin*, 130: 1085–1098.
- Rooney, A.D., Chew, D.M., Selby, D., 2011. Re-Os geochronology of the Neoproterozoic–Cambrian Dalradian Supergroup of Scotland and Ireland: Implications for Neoproterozoic stratigraphy, glaciations and Re-Os systematics. *Precambrian Research*, 185: 202–214.

- Rooney, A.D., Selby, D., Houzay, J.P., Renne, P.R., 2010. Re-Os geochronology of a Mesoproterozoic sedimentary succession, Taoudeni basin, Mauritania: Implications for basin-wide correlations and Re-Os organic-rich sediments systematics. *Earth and Planetary Science Letters*, 289: 486–496.
- Rooney, A.D., Selby, D., Lewan, M.D., Lillis, P.G., Houzay, J.P., 2012. Evaluating Re-Os systematics in organic-rich sedimentary rocks in response to petroleum generation using hydrous pyrolysis experiments. *Geochimica et Cosmochimica Acta*, 77: 275–291.
- Rooney, A.D., Selby, D., Lloyd, J.M., Roberts, D.H., Lückge, A., Sageman, B.B., Prouty, N.G., 2016. Tracking millennial-scale Holocene glacial advance and retreat using osmium isotopes: Insights from the Greenland ice sheet. *Quaternary Science Reviews*, 138: 49–61.
- Schiøler, P., Rogers, K.M., Sykes, R., Hollis, C.J., Ilg, B., Meadows, D., Roncaglia, L., Uruski, C.I., 2010. Palynofacies, organic geochemistry and depositional environment of the Tartan Formation (Late Paleocene), a potential source rock in the Great South Basin, New Zealand. *Marine and Petroleum Geology*, 27: 351–369.
- Schmitz, B., Peucker-Ehrenbrink, B., Heilmann-Clausen, C., Åberg, G., Asaro, F., Lee, C.-T.A., 2004. Basaltic explosive volcanism, but no comet impact, at the Paleocene–Eocene boundary: high-resolution chemical and isotopic records from Egypt, Spain and Denmark. *Earth and Planetary Science Letters*, 225: 1–17.
- Selby, D., 2007. Direct Rhenium-Osmium age of the Oxfordian-Kimmeridgian boundary, Staffin bay, Isle of Skye, U.K., and the late Jurassic time scale. *Norsk Geologisk Tidsskrift*, 87: 291–299.
- Selby, D., Creaser, R.A., 2003. Re-Os geochronology of organic rich sediments: an evaluation of organic matter analysis methods. *Chemical Geology*, 200: 225–240.
- Selby, D., Creaser, R.A., 2005a. Direct radiometric dating of hydrocarbon deposits using rhenium-osmium isotopes. *Science*, 308: 1293–1295.
- Selby, D., Creaser, R.A., 2005b. Direct radiometric dating of the Devonian-Mississippian time-scale boundary using the Re-Os black shale geochronometer. *Geology*, 33: 545.
- Selby, D., Creaser, R.A., Stein, H.J., Markey, R.J., Hannah, J.L., 2007. Assessment of the ^{187}Re decay constant by cross calibration of Re-Os molybdenite and U-Pb zircon chronometers in magmatic ore systems. *Geochimica et Cosmochimica Acta*, 71: 1999–2013.
- Selby, D., Mutterlose, J., Condon, D.J., 2009. U-Pb and Re-Os geochronology of the Aptian/Albian and Cenomanian/Turonian stage boundaries: Implications for timescale calibration, osmium isotope seawater composition and Re-Os systematics in organic-rich sediments. *Chemical Geology*, 265: 394–409.
- Smoliar, M.I., Walker, R.J., Morgan, J.W., 1996. Re-Os Ages of Group IIA, IIIA, IVA, and IVB Iron Meteorites. *Science*, 271: 1099–1102.
- Sun, W., Bennett, V.C., Eggins, S.M., Kamenetsky, V.S., Arculus, R.J., 2003. Enhanced mantle-to-crust rhenium transfer in undegassed arc magmas. *Nature*, 422: 294.
- Taylor, M.J.S., 2011. Investigating stratigraphic evidence for Antarctic glaciation in the greenhouse world of the Paleocene, eastern North Island, New Zealand. Masters Thesis, University of Waikato.

- Them, T.R., Gill, B.C., Selby, D., Gröcke, D.R., Friedman, R.M., Owens, J.D., 2017. Evidence for rapid weathering response to climatic warming during the Toarcian Oceanic Anoxic Event. *Scientific Reports*, 7: 5003.
- Thomas, D.J., Bralower, T.J., Jones, C.E., 2003. Neodymium isotopic reconstruction of late Paleocene–early Eocene thermohaline circulation. *Earth and Planetary Science Letters*, 209: 309–322.
- Tissot, B.P., Welte, D.H., 1984. *Petroleum Formation and Occurrence*. Springer-Verlag, Berlin, 699 pp.
- Torsvik, T.H., Van der Voo, R., Preeden, U., Mac Niocaill, C., Steinberger, B., Doubrovine, P.V., van Hinsbergen, D.J.J., Domeier, M., Gaina, C., Tohver, E., Meert, J.G., McCausland, P.J.A., Cocks, L.R.M., 2012. Phanerozoic polar wander, palaeogeography and dynamics. *Earth-Science Reviews*, 114: 325–368.
- Tripathy, G.R., Hannah, J.L., Stein, H.J., 2018. Refining the Jurassic-Cretaceous boundary: Re-Os geochronology and depositional environment of Upper Jurassic shales from the Norwegian Sea. *Palaeogeography, Palaeoclimatology, Palaeoecology*, 503: 13–25.
- Tripathy, G.R., Hannah, J.L., Stein, H.J., Geboy, N.J., Ruppert, L.F., 2015. Radiometric dating of marine-influenced coal using Re-Os geochronology. *Earth and Planetary Science Letters*, 432: 13–23.
- Turgeon, S.C., Creaser, R.A., Algeo, T.J., 2007. Re-Os depositional ages and seawater Os estimates for the Frasnian–Famennian boundary: Implications for weathering rates, land plant evolution, and extinction mechanisms. *Earth and Planetary Science Letters*, 261: 649–661.
- van Acken, D., Tütken, T., Daly, J.S., Schmid-Röhl, A., Orr, P.J., 2019. Rhenium-osmium geochronology of the Toarcian Posidonia Shale, SW Germany. *Palaeogeography, Palaeoclimatology, Palaeoecology*, 534: 109294.
- Westerhold, T., Röhl, U., Donner, B., McCarren, H.K., Zachos, J.C., 2011. A complete high-resolution Paleocene benthic stable isotope record for the central Pacific (ODP Site 1209). *Paleoceanography*, 26: PA2216.
- Westerhold, T., Röhl, U., Donner, B., Zachos, J.C., 2018. Global extent of early Eocene hyperthermal events: A new Pacific benthic foraminiferal isotope record from Shatsky Rise (ODP Site 1209). *Paleoceanography and Paleoclimatology*, 33: 626–642.
- Westerhold, T., Röhl, U., Frederichs, T., Agnini, C., Raffi, I., Zachos, J.C., Wilkens, R.H., 2017. Astronomical calibration of the Ypresian timescale: implications for seafloor spreading rates and the chaotic behavior of the solar system? *Climate of the Past*, 13: 1129–1152.
- Wieczorek, R., Fantle, M.S., Kump, L.R., Ravizza, G., 2013. Geochemical evidence for volcanic activity prior to and enhanced terrestrial weathering during the Paleocene Eocene Thermal Maximum. *Geochimica et Cosmochimica Acta*, 119: 391–410.
- Wilson, G.J., Moore, P.R., 1988. Cretaceous-Tertiary boundary in the Te Hoe River area, western Hawkes Bay. *New Zealand Geological Survey Record*, 35: 34–37.
- Woodhouse, O.B., Ravizza, G., Kenison Falkner, K., Statham, P.J., Peucker-Ehrenbrink, B., 1999. Osmium in seawater: vertical profiles of concentration and isotopic composition in the eastern Pacific Ocean. *Earth and Planetary Science Letters*, 173: 223–233.

- Xu, G., Hannah, J.L., Stein, H.J., Bingen, B., Yang, G., Zimmerman, A., Weitschat, W., Mørk, A., Weiss, H.M., 2009. Re-Os geochronology of Arctic black shales to evaluate the Anisian-Ladinian boundary and global faunal correlations. *Earth and Planetary Science Letters*, 288: 581–587.
- Xu, W., Ruhl, M., Jenkyns, Hugh C., Hesselbo, Stephen P., Riding, James B., Selby, D., Naafs, B.David A., Weijers, Johan W.H., Pancost, Richard D., Tegelaar, Erik W., Idiz, Erdem F., 2017. Carbon sequestration in an expanded lake system during the Toarcian oceanic anoxic event. *Nature Geoscience*, 10: 129.
- Yamashita, Y., Takahashi, Y., Haba, H., Enomoto, S., Shimizu, H., 2007. Comparison of reductive accumulation of Re and Os in seawater–sediment systems. *Geochimica et Cosmochimica Acta*, 71: 3458-3475.
- Yang, G., Hannah, J.L., Zimmerman, A., Stein, H.J., Bekker, A., 2009. Re-Os depositional age for Archean carbonaceous slates from the southwestern Superior Province: Challenges and insights. *Earth and Planetary Science Letters*, 280: 83–92.
- Zachos, J.C., Dickens, G.R., Zeebe, R.E., 2008. An early Cenozoic perspective on greenhouse warming and carbon-cycle dynamics. *Nature*, 451: 279.
- Zhu, B., Becker, H., Jiang, S.Y., Pi, D.H., Fischer-Gödde, M., Yang, J.H., 2013. Re-Os geochronology of black shales from the Neoproterozoic Doushantuo Formation, Yangtze platform, South China. *Precambrian Research*, 225: 67–76.

Fig. 1
[Click here to download high resolution image](#)

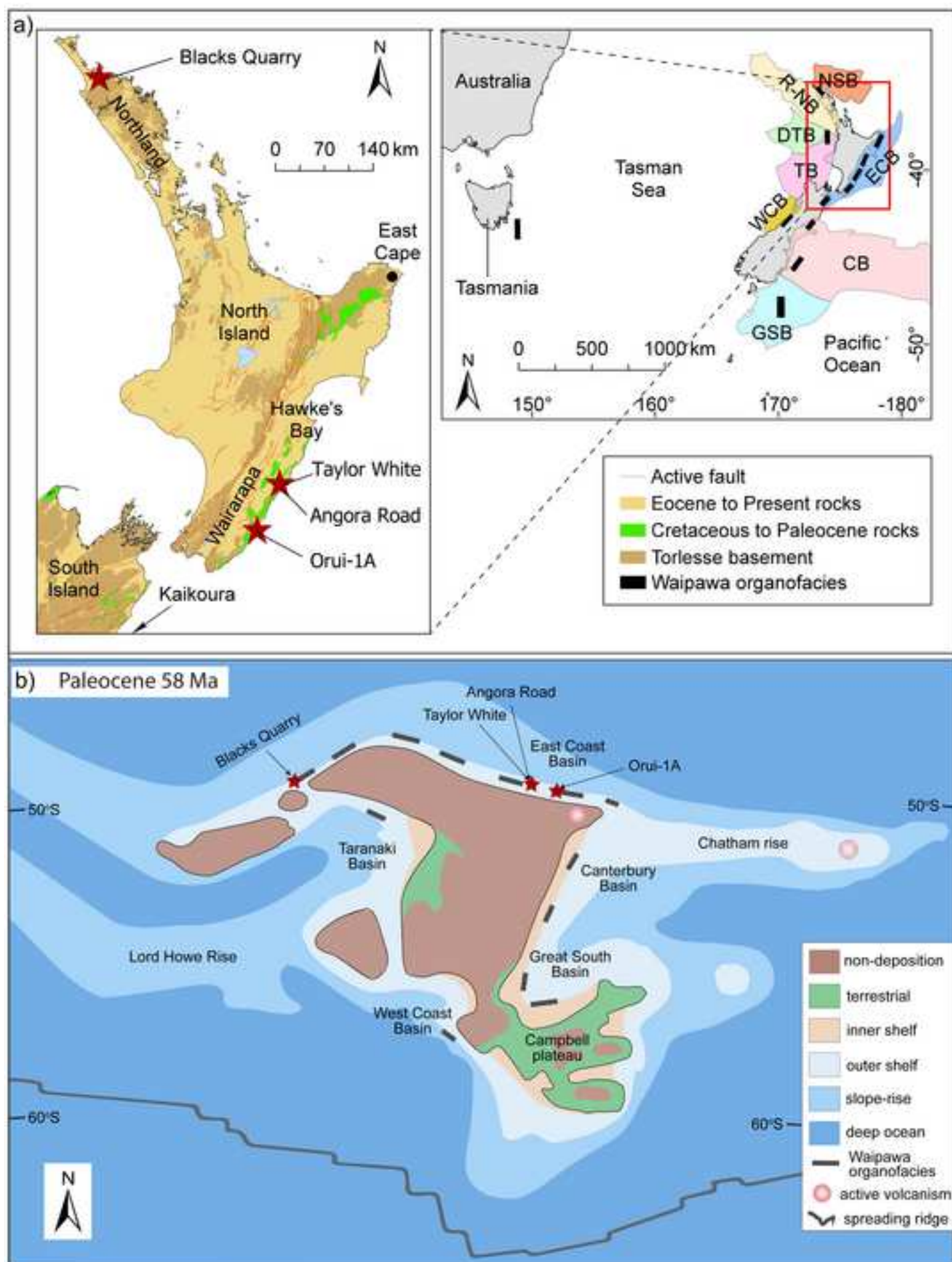


Fig. 2
[Click here to download high resolution image](#)

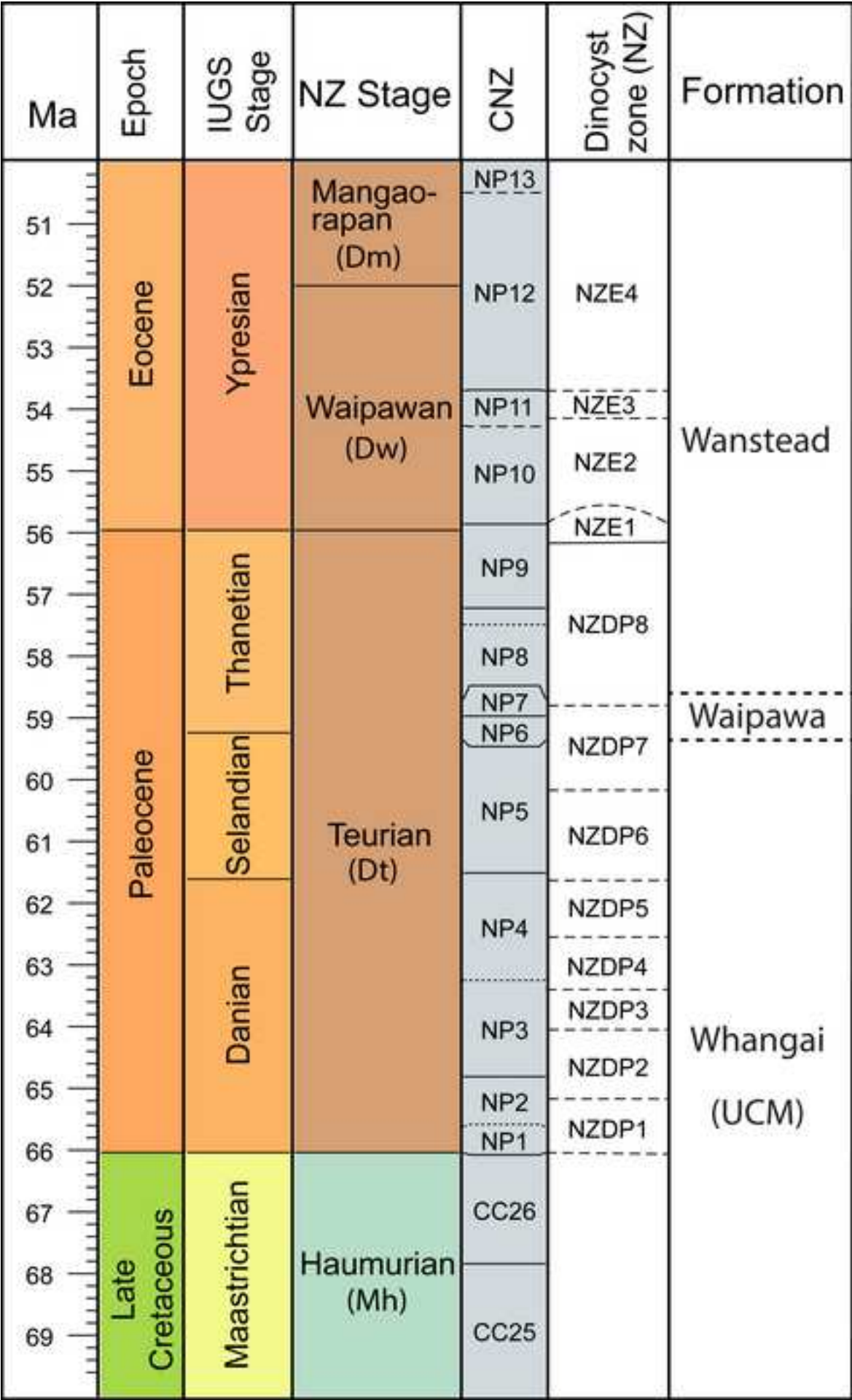


Fig. 3

[Click here to download high resolution image](#)

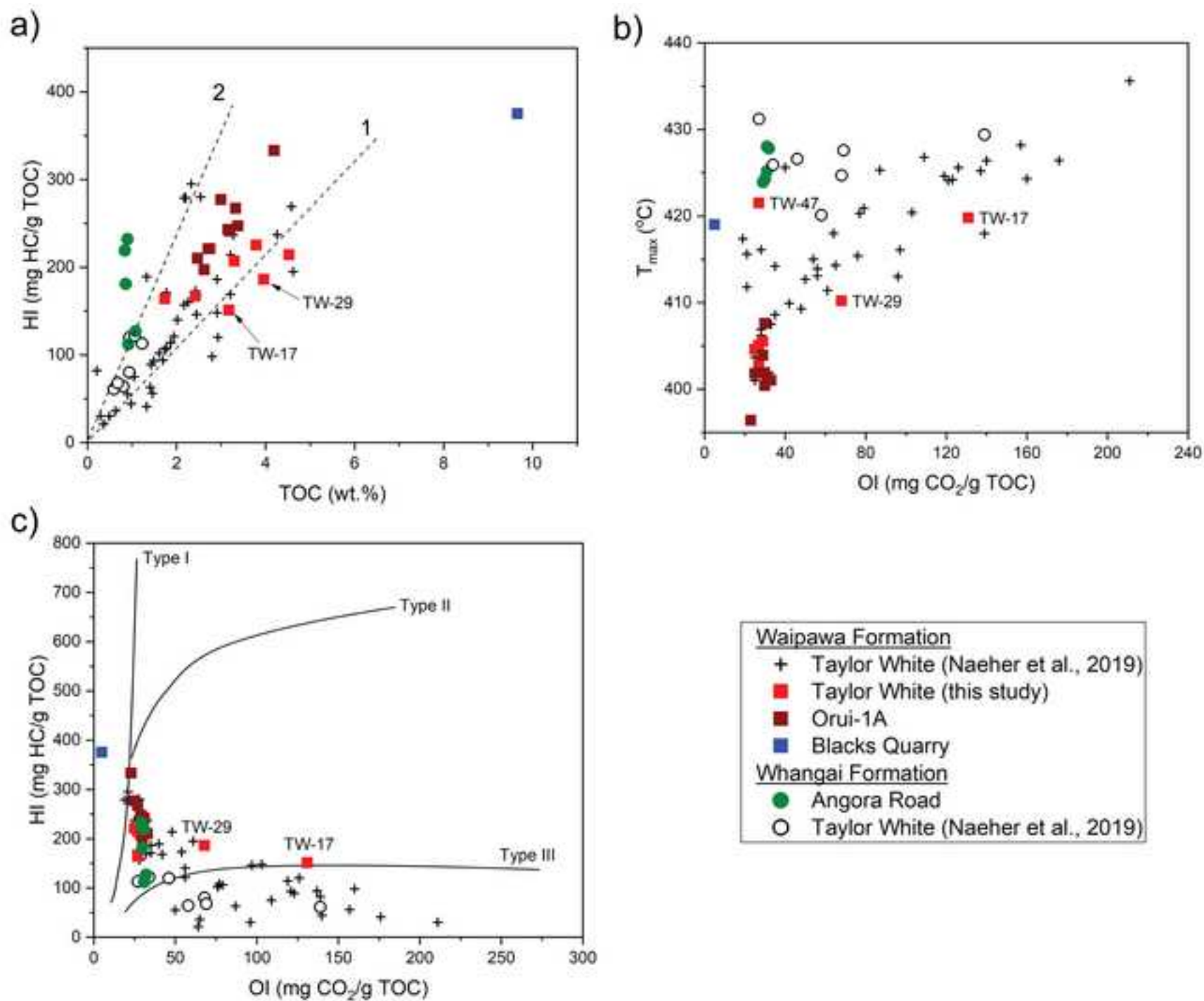


Fig. 4

[Click here to download high resolution image](#)

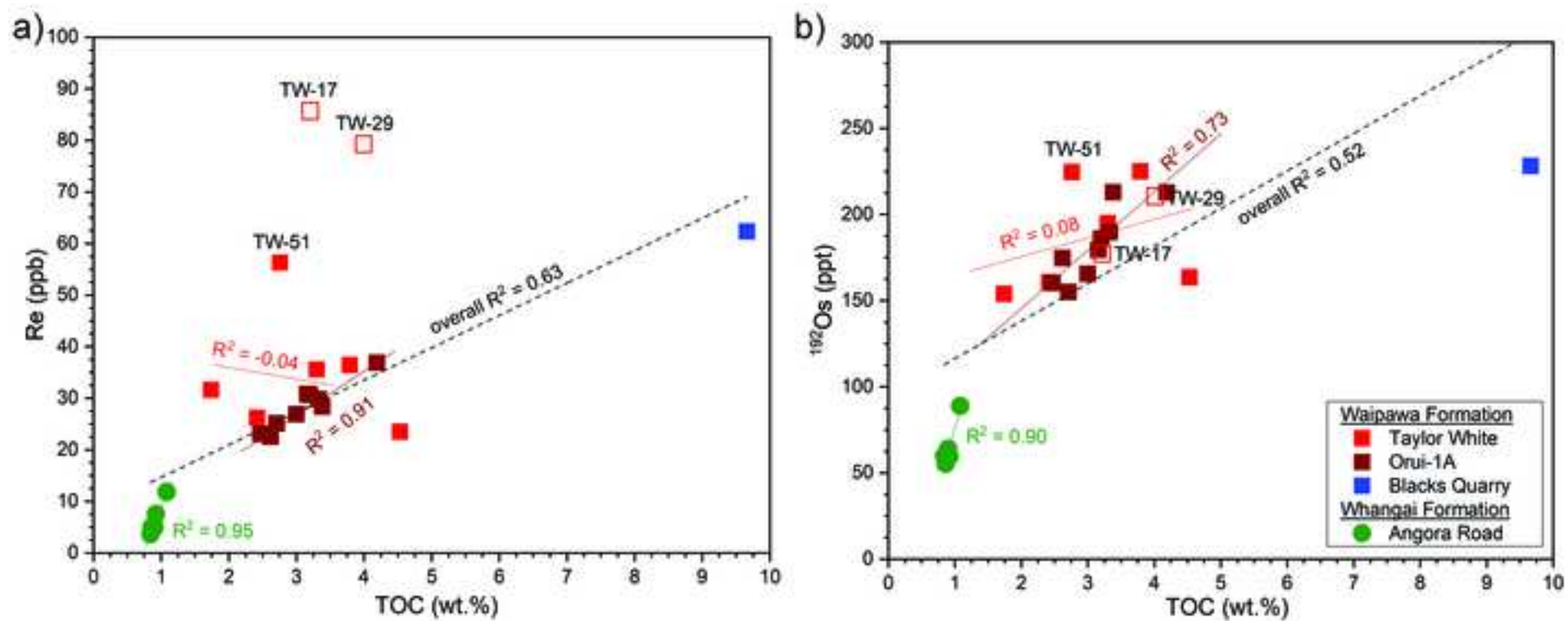


Fig. 5

[Click here to download high resolution image](#)

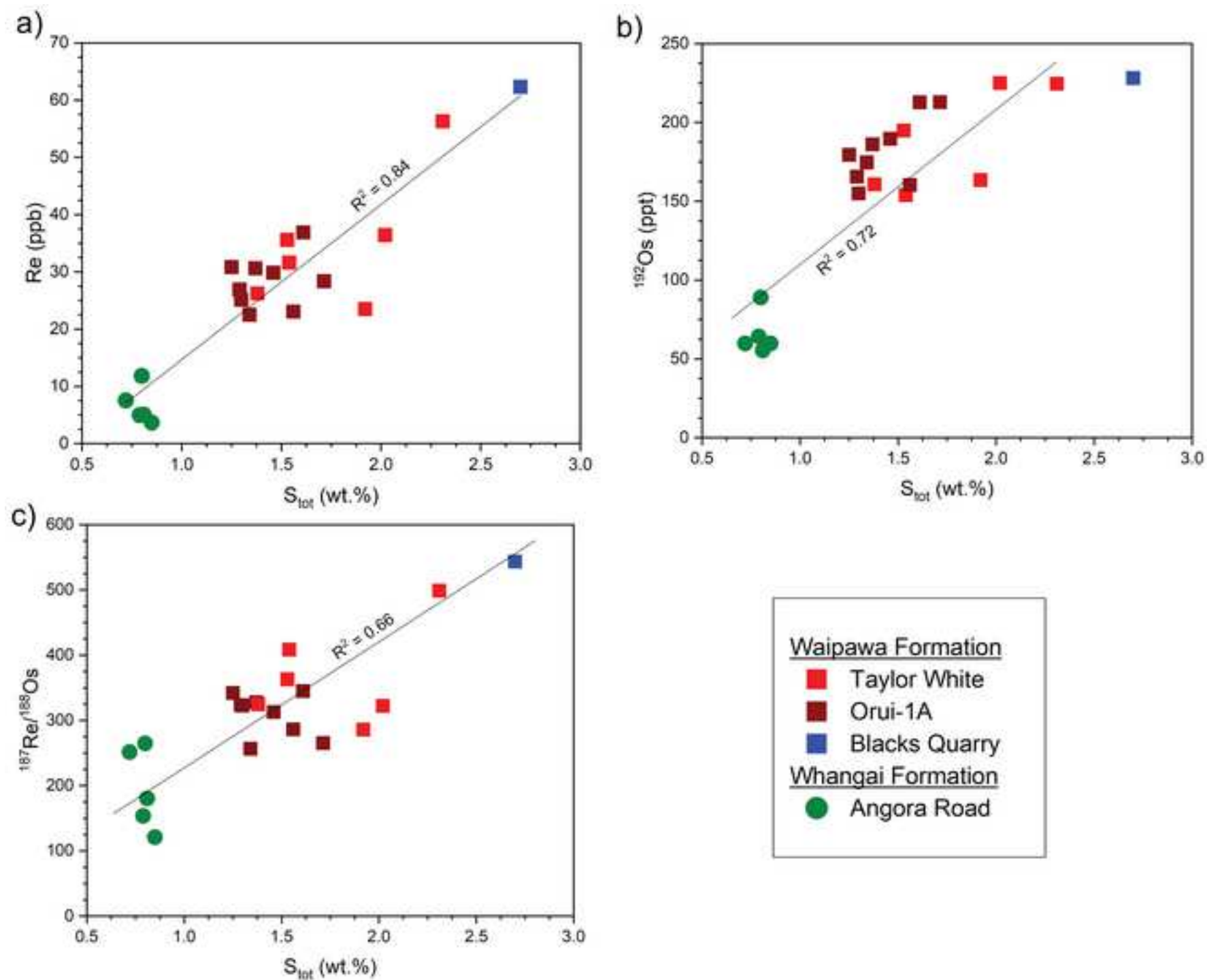


Fig. 6
[Click here to download high resolution image](#)

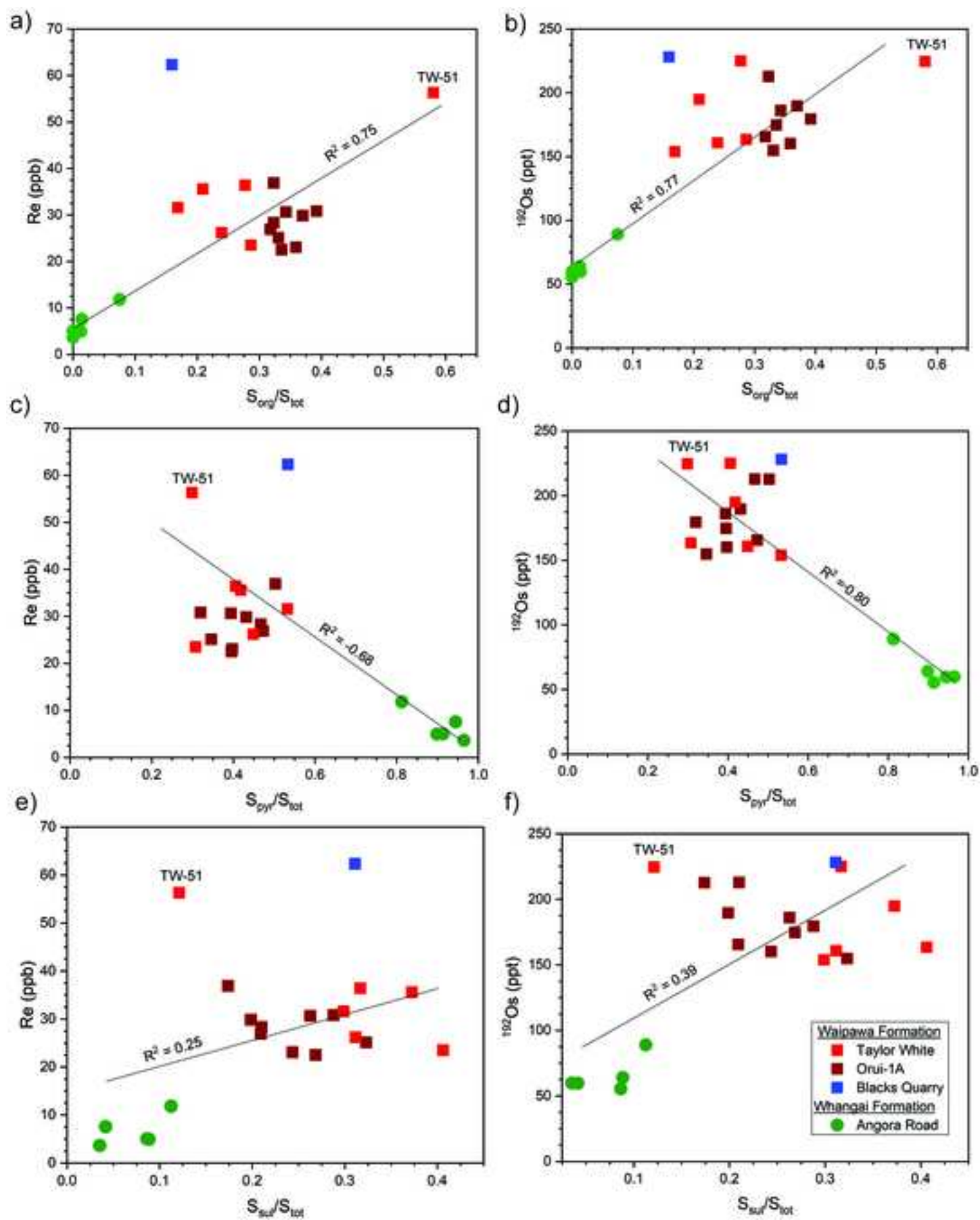


Fig. 7

[Click here to download high resolution image](#)

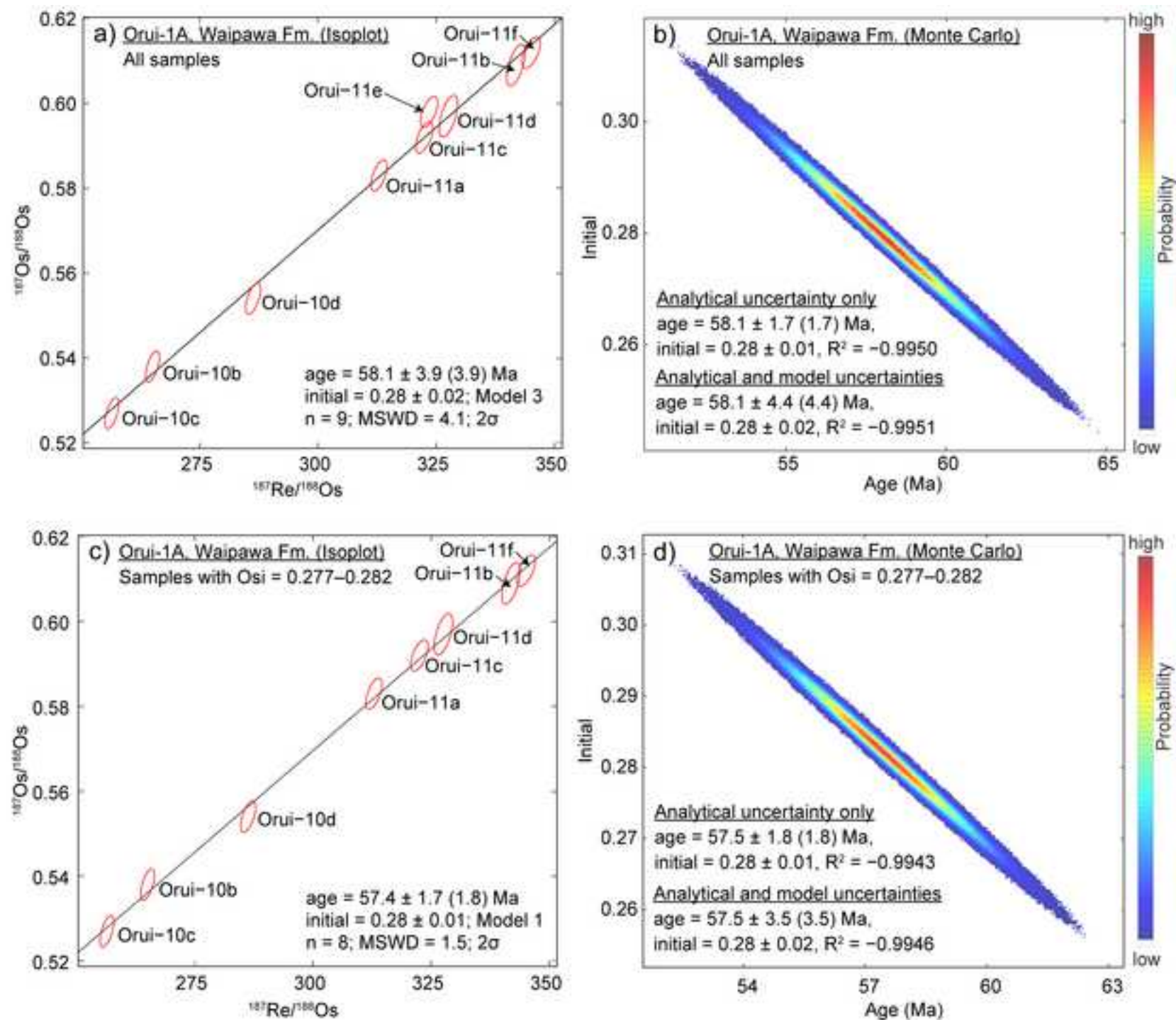


Fig. 8

[Click here to download high resolution image](#)

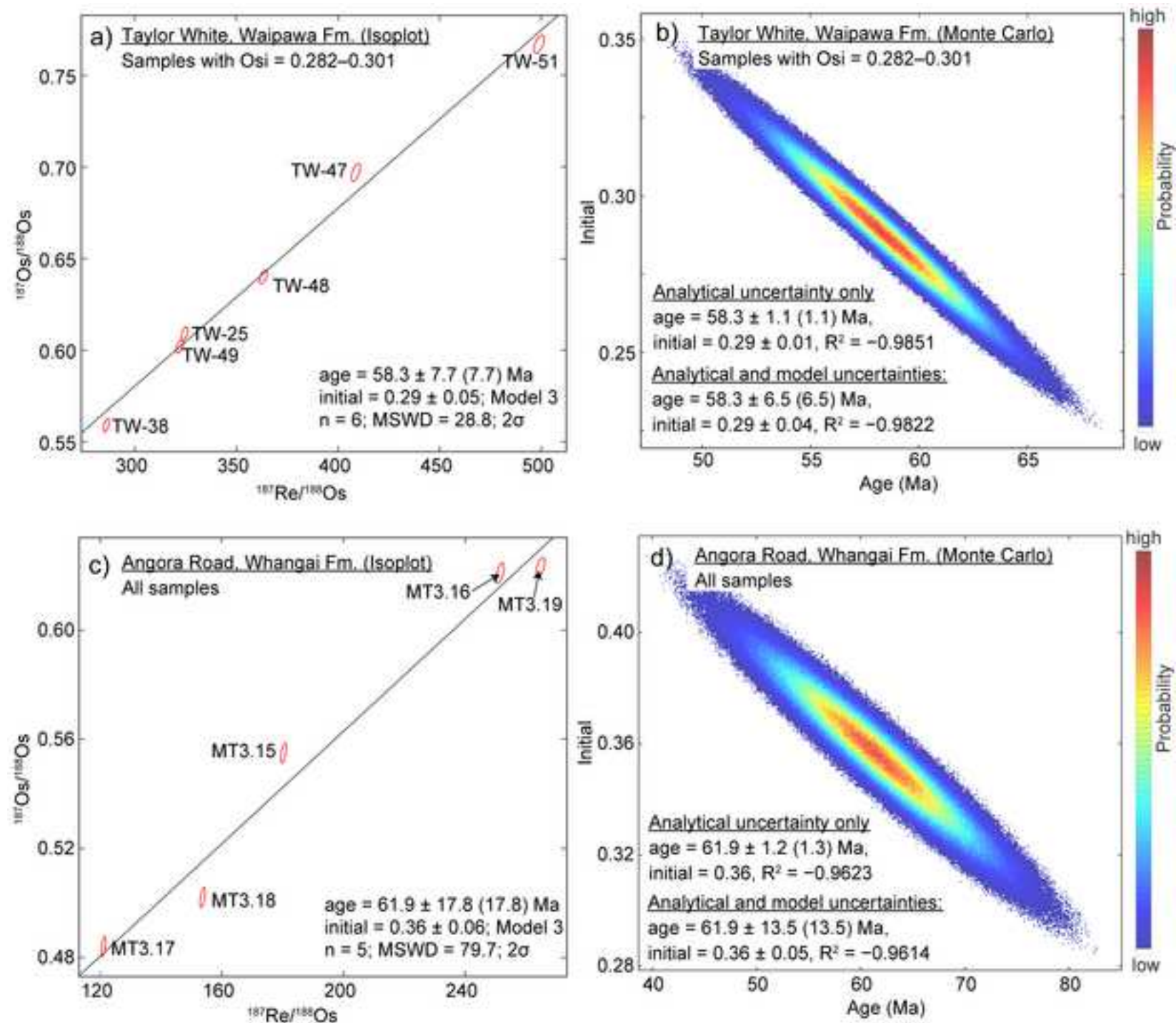


Fig. 9

[Click here to download high resolution image](#)

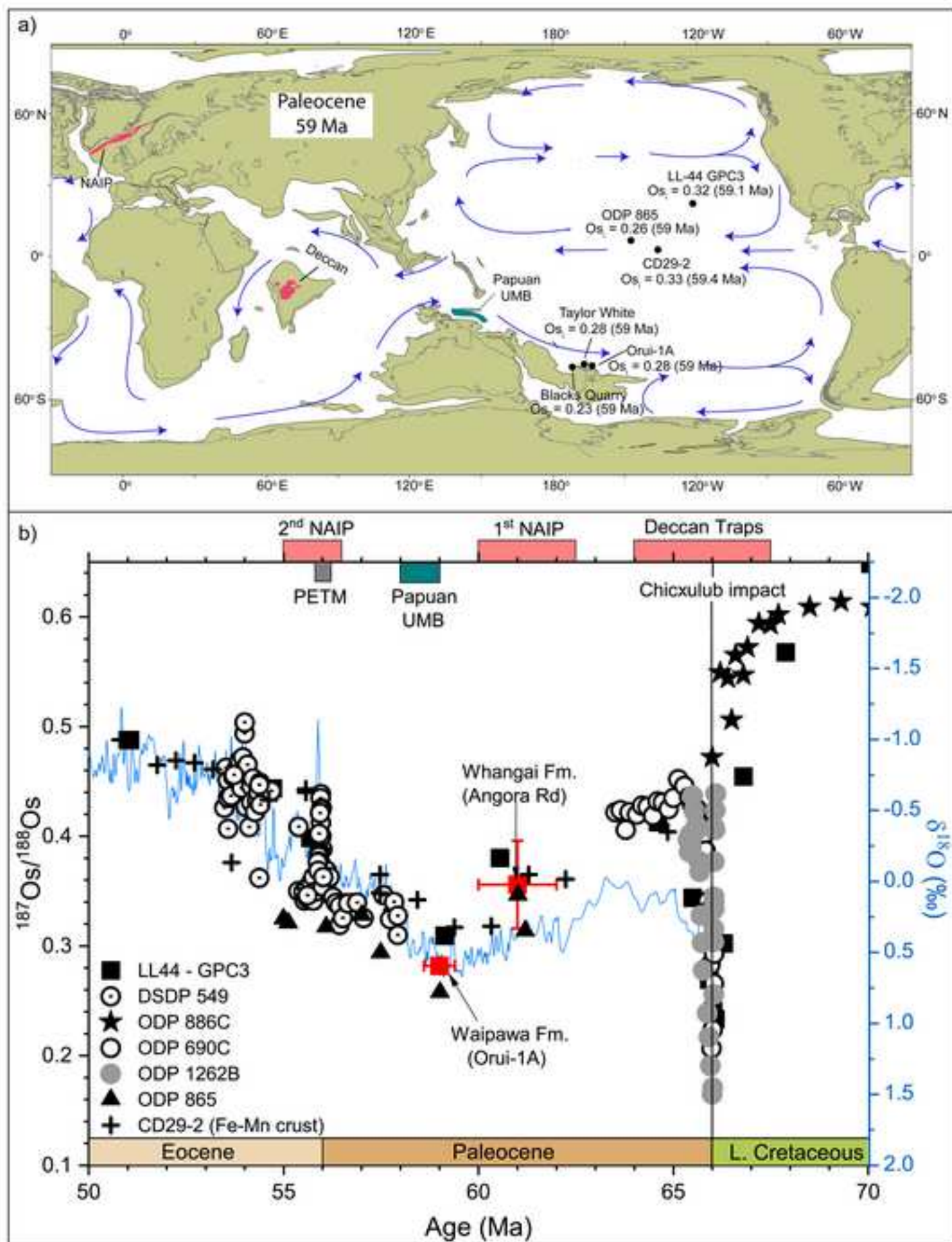


Fig. 10

[Click here to download high resolution image](#)

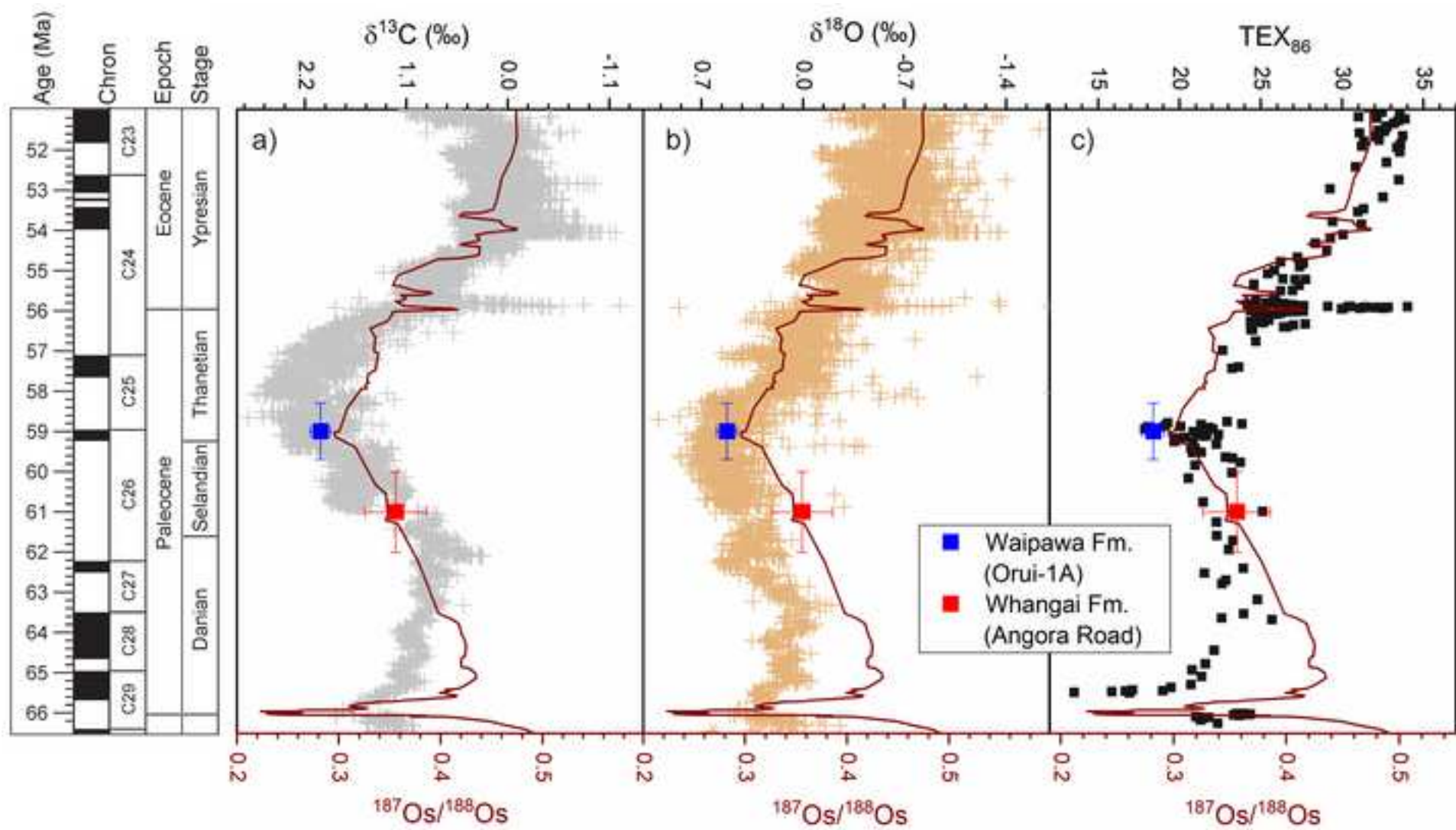


Table 1: Bulk pyrolysis and sulphur data for the Waipawa and Whangai formation samples.

Sample ID	*Height/depth (m)	TOC (wt.%)	T _{max} (°C)	S1	S2	HI (mg HC/ g TOC)	OI (mg CO ₂ / g TOC)	S _{tot}	S _{sul}	S _{pyr}	S _{org}	S _{sul} /S _{tot}	S _{pyr} /S _{tot}	S _{org} /S _{tot}
				(mg HC/g rock)				(wt.%)						
<u>Orui-1A core – Waipawa Fm.</u>														
Orui-10b	48.4	3.4	404	0.16	8.4	247	29	1.71	0.36	0.80	0.55	0.21	0.47	0.32
Orui-10c	48.8	2.6	408	0.14	5.2	197	30	1.34	0.36	0.53	0.45	0.27	0.40	0.34
Orui-10d	49.5	2.5	401	0.15	5.2	210	33	1.56	0.38	0.62	0.56	0.24	0.40	0.36
Orui-11a	49.9	3.3	402	0.21	8.9	267	27	1.46	0.29	0.63	0.54	0.20	0.43	0.37
Orui-11b	50.2	3.2	402	0.25	7.7	243	30	1.25	0.36	0.40	0.49	0.29	0.32	0.39
Orui-11c	50.4	2.7	400	0.16	6.0	221	30	1.30	0.42	0.45	0.43	0.32	0.35	0.33
Orui-11d	50.9	3.2	401	0.19	7.7	241	31	1.37	0.36	0.54	0.47	0.26	0.39	0.34
Orui-11e	51.1	3.0	402	0.15	8.3	277	25	1.29	0.27	0.61	0.41	0.21	0.47	0.32
Orui-11f	51.6	4.2	396	0.28	13.9	333	23	1.61	0.28	0.81	0.52	0.17	0.50	0.32
<u>Taylor White section – Waipawa Fm.</u>														
TW-51	138.0	2.8	405	0.14	6.1	221	25	2.31	0.28	0.69	1.34	0.12	0.30	0.58
TW-49	135.5	3.8	405	0.13	8.5	225	27	2.02	0.64	0.82	0.56	0.32	0.41	0.28
TW-48	134.0	3.3	406	0.07	6.8	207	29	1.53	0.57	0.64	0.32	0.37	0.42	0.21
TW-47	132.5	1.7	422	0.04	2.9	164	27	1.54	0.46	0.82	0.26	0.30	0.53	0.17
TW-38	119.0	4.5	405	0.16	9.7	214	27	1.92	0.78	0.59	0.55	0.41	0.31	0.29
TW-29	105.5	4.0	410	0.11	7.4	186	68	1.21	0.27	0.60	0.34	0.22	0.50	0.28
TW-25	99.5	2.4	403	0.10	4.0	167	27	1.38	0.43	0.62	0.33	0.31	0.45	0.24
TW-17	87.5	3.2	420	0.17	4.8	151	131	0.28	0.10	0.09	0.09	0.36	0.32	0.32
<u>Blacks Quarry – Waipawa Fm.</u>														
BQ02	–	9.7	419	3.35	36.3	375	5	2.70	0.84	1.44	0.43	0.31	0.53	0.16
<u>Angora Road – Whangai Fm.</u>														
MT3.19	34.6	1.1	428	0.01	1.4	127	32	0.80	0.09	0.65	0.06	0.11	0.81	0.08
MT3.18	29.0	0.9	424	0.02	2.1	232	29	0.79	0.07	0.71	0.01	0.09	0.90	0.01
MT3.17	25.4	0.8	425	0.01	1.9	219	31	0.85	0.03	0.82	0.00	0.04	0.96	0.00
MT3.16	21.8	0.9	428	0.01	1.0	112	31	0.72	0.03	0.68	0.01	0.04	0.94	0.01
MT3.15	17.8	0.9	424	0.01	1.6	181	30	0.81	0.07	0.74	0.00	0.09	0.91	0.00

* Stratigraphic height for outcrop samples and drill-hole depth for the core samples.

Table 2: Re and Os concentrations and isotope data for the Waipawa and Whangai formation samples.

Sample ID	*Height/depth (m)	Re (ppb)	±	Os (ppt)	±	¹⁹² Os (ppt)	±	¹⁸⁷ Re/ ¹⁸⁸ Os	±	¹⁸⁷ Os/ ¹⁸⁸ Os	±	rho	Os _i ^a (58 Ma)	Os _i ^b (59 Ma)
<u>Orui-1A - Waipawa Fm.</u>														
Orui-10b	48.4	28.35	0.07	543.1	1.7	212.8	0.8	265.0	1.2	0.538	0.003	0.598	0.282	0.278
Orui-10c	48.8	22.51	0.06	445.1	1.4	174.7	0.7	256.4	1.2	0.527	0.003	0.600	0.279	0.275
Orui-10d	49.5	23.07	0.06	409.8	1.3	160.2	0.6	286.3	1.3	0.554	0.003	0.600	0.277	0.272
Orui-11a	49.9	29.83	0.07	486.7	1.6	189.7	0.7	312.9	1.4	0.583	0.003	0.601	0.281	0.276
Orui-11b	50.2	30.84	0.08	461.9	1.6	179.4	0.7	341.9	1.6	0.609	0.004	0.593	0.279	0.273
Orui-11c	50.4	25.11	0.06	397.9	1.3	154.9	0.6	322.5	1.5	0.592	0.003	0.601	0.280	0.275
Orui-11d	50.9	30.64	0.08	478.2	1.6	186.0	0.8	327.6	1.6	0.597	0.004	0.583	0.281	0.275
Orui-11e	51.1	26.91	0.07	425.5	1.4	165.5	0.7	323.5	1.5	0.598	0.003	0.599	0.286	0.280
Orui-11f	51.6	36.89	0.09	547.8	1.8	212.7	0.8	345.1	1.6	0.612	0.003	0.596	0.279	0.273
<u>Taylor White - Waipawa Fm.</u>														
TW-51	138.0	56.31	0.14	589.3	1.9	224.5	0.8	498.9	2.1	0.767	0.004	0.574	0.285	0.276
TW-51 (rpt)	138.0	56.26	0.14	587.2	1.9	223.2	0.8	496.7	2.0	0.764	0.004	0.571	0.284	0.276
TW-49	135.5	36.42	0.09	578.7	1.8	225.0	0.8	322.1	1.4	0.602	0.003	0.570	0.291	0.285
TW-49 (rpt)	135.5	36.35	0.09	651.1	1.9	254.9	0.9	283.7	1.2	0.545	0.003	0.564	0.271	0.266
TW-48	134.0	35.58	0.09	503.6	1.6	194.9	0.7	363.2	1.6	0.640	0.003	0.586	0.289	0.283
TW-47	132.5	31.60	0.08	400.2	1.3	153.8	0.6	408.7	1.8	0.697	0.004	0.584	0.301	0.295
TW-38	119.0	23.51	0.06	418.3	1.3	163.5	0.6	286.0	1.2	0.559	0.003	0.571	0.282	0.278
TW-29	105.5	72.92	0.18	538.7	1.6	210.7	0.7	688.4	2.9	0.551	0.003	0.570	-0.114	-0.126
TW-25	99.5	26.21	0.06	413.7	1.3	160.7	0.6	324.5	1.4	0.609	0.003	0.582	0.296	0.290
TW-17	87.5	85.86	0.21	455.4	1.4	177.3	0.6	963.2	4.0	0.588	0.003	0.571	-0.343	-0.359
<u>Blacks Quarry – Waipawa Fm.</u>														
BQ02	—	62.32	0.15	598.6	2.1	228.2	0.8	543.4	2.4	0.764	0.004	0.572	0.239	0.230
<u>Angora Road - Whangai Fm.</u>														
MT3.19	34.6	11.83	0.03	228.1	0.7	89.0	0.3	264.7	1.2	0.623	0.003	0.584	(62 Ma)	
MT3.18	29.0	4.95	0.01	162.9	0.5	64.1	0.3	153.7	0.7	0.502	0.003	0.599		
MT3.17	25.4	3.64	0.01	151.7	0.5	59.8	0.3	121.1	0.6	0.484	0.003	0.609		
MT3.16	21.8	7.55	0.02	153.9	0.5	59.7	0.2	251.5	1.1	0.621	0.003	0.593		
MT3.15	17.8	5.02	0.01	141.8	0.5	55.4	0.2	180.3	0.8	0.555	0.003	0.597		

All uncertainties are stated at 2σ . Rho is the associated error correlation

rpt = replicate analysis on sample splits of the same sample powder

*Stratigraphic height for outcrop samples and drill-hole depth for the core samples

^aInitial $^{187}\text{Os}/^{188}\text{Os}$ values calculated at 58 Ma for the Waipawa Formation and 62 Ma for the Whangai Formation using the ^{187}Re decay constant of $1.666 \times 10^{-11} \text{ a}^{-1}$ (Smoliar et al., 1996)

^bInitial $^{187}\text{Os}/^{188}\text{Os}$ values calculated at 59 Ma for the Waipawa Formation

Supplementary online material

[Click here to download Background dataset for online publication only: Supplementary information.doc](#)

Declaration of interests

☒ The authors declare that they have no known competing financial interests or personal relationships that could have appeared to influence the work reported in this paper.

☐ The authors declare the following financial interests/personal relationships which may be considered as potential competing interests: